

# A Total-Group Phylogenetic Metatree for Cetacea and the Importance of Fossil Data in Diversification Analyses

GRAEME T. LLOYD<sup>1,\*</sup>, GRAHAM J. SLATER<sup>2</sup>

<sup>1</sup> *School of Earth and Environment, University of Leeds, Leeds, U.K.*

<sup>2</sup> *Department of the Geophysical Sciences, University of Chicago, Chicago 60637, USA*

*\*graemetlloyd@gmail.com*

## ABSTRACT

1 Phylogenetic trees provide a powerful framework for testing macroevolutionary hypotheses,  
2 but it is becoming increasingly apparent that inferences derived from extant species alone  
3 can be highly misleading. Trees incorporating living and extinct taxa are needed to  
4 address fundamental questions about the origins of diversity and disparity but it has  
5 proved challenging to generate robust, species-rich phylogenies that include large numbers  
6 of fossil taxa. As a result, most studies of diversification dynamics continue to rely on  
7 molecular phylogenies. Here, we extend and apply a recently developed meta-analytic  
8 approach for synthesizing previously published phylogenetic studies to infer a well-resolved  
9 set of species level, time-scaled phylogenetic hypotheses for extinct and extant cetaceans  
10 (whales, dolphins and allies). Our trees extend sampling from the ~ 90 extant species to  
11 over 400 living and extinct species, and therefore allow for more robust inference of  
12 macroevolutionary dynamics. While the diversification scenarios we recover are broadly  
13 concordant with those inferred from molecular phylogenies they differ in critical ways,  
14 most notably in the relative contributions of extinction and speciation rate shifts in driving  
15 rapid radiations. Supertrees are often viewed as poor substitute for phylogenies inferred  
16 directly from character data but the metatree pipeline overcomes many of the past

17 criticisms leveled at these approaches. Meta-analytic phylogenies provide the most  
18 immediate route for integrating fossils into macroevolutionary analyses, the results of  
19 which range from untrustworthy to nonsensical without them.

20 *Key words:* supertree, morphology, matrix representation with parsimony, extinction,  
21 macroevolution.

22

23 It is now widely accepted that a phylogenetic framework is essential for addressing  
24 questions regarding diversification dynamics, phenotypic evolution, and historical  
25 biogeography. The covariances between species that are imposed by the hierarchical  
26 structure of a phylogenetic tree mean that any attempt to understand the processes  
27 responsible for generating observed patterns of diversity must take the tree and its  
28 associated branch lengths into account (Felsenstein, 1985; Harvey and Pagel, 1991; Foote,  
29 1996; O'Meara et al., 2006; Ree and Smith, 2008). As a consequence of this phylogenetic  
30 dependence, the development of new tools for inferring macroevolutionary dynamics has  
31 been paralleled by innovations in the field of phylogenetic inference, and it is now possible  
32 to infer time-scaled trees using complex models of molecular evolution applied to  
33 genome-scale data.

34 The need for a well-resolved, time-calibrated phylogeny places substantial  
35 constraints on the kinds of clades that are accessible to most biologists for testing  
36 macroevolutionary hypotheses. Some authors have noted that clades are often selected for  
37 study due to their tractability rather than because they are suitable candidates for testing  
38 a particular hypothesis, resulting in a form of empirical ascertainment bias (Beaulieu and  
39 O'Meara, 2018, 2019). For example, early burst models of adaptive radiation arose to  
40 explain the origins of higher taxa (Simpson, 1944, 1953; Van Valen, 1971; Valentine, 1980;  
41 Humphreys and Barraclough, 2014; Slater and Friscia, 2019) but have mostly been tested  
42 in lower level clades, such as genera, where the early burst signal is conspicuously lacking

43 (e.g., [Harmon et al., 2010](#)). Although lower level clades certainly have a role to play in  
44 comparative biology ([Schluter 2000](#); [Losos, 2009](#); [Donoghue and Edwards, 2019](#)), there is a  
45 pressing need to develop suitable phylogenetic frameworks for studying macroevolutionary  
46 pattern and process at higher taxonomic levels.

47 The major barrier to obtaining appropriate phylogenetic frameworks for higher-level  
48 clades has always been data availability ([Smith et al., 2009](#)). The “Supermatrix” approach  
49 was initially suggested as a solution to this problem ([Sanderson et al., 1998](#); [Gatesy et al.,](#)  
50 [2002](#); [de Queiroz and Gatesy, 2007](#)). Here, one obtains all available sequence data for a  
51 clade of interest through a combination of direct sequencing and from repositories such as  
52 Genbank. Sequences are aligned and concatenated to create a large but sparsely sampled  
53 matrix that can be analyzed using standard phylogenetic software and methods. Concerns  
54 regarding the impact of missing data and data quality (e.g., [McMahon and Sanderson](#)  
55 [2006](#)) have, more recently, led to alternative approaches based on bioinformatic pipelines  
56 [Smith et al. \(2009\)](#) or patching of subclades onto backbone trees ([Jetz et al., 2012](#); [Tonini](#)  
57 [et al., 2016](#); [Jetz and Pyron, 2018](#); [Upham et al., 2019](#)). These methods have proved  
58 effective for generating large, higher-level phylogenetic hypotheses (particularly where  
59 taxonomic information can also be used to constrain the placement of species that lack  
60 character data) and have yielded novel insights into diversification dynamics, trait  
61 evolution and historical biogeographic patterns. Recent examples include a 5,284 species  
62 tree of agariomycete fungi ([Varga et al., 2019](#)), an 11,638 species tree of extant fishes  
63 ([Rabosky et al., 2018](#)), and a 353,185 species tree of seed plants ([Smith and Brown, 2018](#)).

64 While these methods provide promise for extant clades, they cannot be used to  
65 generate phylogenetic hypotheses for most of the > 99% of life that is now extinct ([Raup](#)  
66 [1994](#)). This is particularly problematic given that fossil data play a critical role in refining  
67 estimates of ancestral character states ([Finarelli and Flynn, 2006](#)), choosing among  
68 competing models of trait evolution ([Slater et al., 2012](#)), inferring ancestral biogeographic  
69 patterns ([Meseguer et al., 2014](#)), and understanding speciation and extinction dynamics

70 through time (Mitchell et al., 2018; Louca and Pennell, 2020). The difficulty in generating  
71 large character–taxon matrices for fossil taxa is due in large part to the unique and often  
72 subjective ways in which morphological characters and their states are defined and coded  
73 across studies. Unlike molecular data, where character states are universally coded, two  
74 morphological matrices with partially overlapping taxon lists cannot be concatenated  
75 without extensive revision of characters and re–coding of their states, which is, in itself, a  
76 challenging, time–consuming, and potentially impossible task. The effect of this  
77 incompatibility is that, although the number of species included in morphological  
78 character–taxon matrices has continued to increase over the past few decades (fig 1), they  
79 lag well behind molecular datasets in size. One recent study included character state  
80 codings for 501 OTUs (Hartman et al., 2019), but this is twice the size of the next largest  
81 matrix published to date (N=254, Mo et al., 2012).

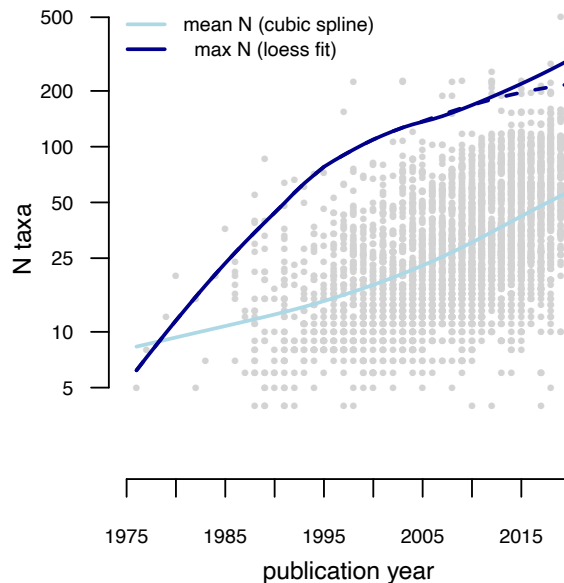


Fig. 1. Although the number of taxa included in morphological character–taxon matrices has increased over time, they lag behind the largest molecular datasets. Based on a cubic spline (light blue line) fitted to  $\log(\text{number of taxa})$  in 3671 morphological studies ([graemetlloyd.com/matr.heml](http://graemetlloyd.com/matr.heml)), the average dataset has only increased from 8.3 OTUs in 1975 to 58 OTUs in 2020 (note log scale on y–axis). The maximum number of taxa has also increased, corroborated by a loess fit (dark blue solid line). Removing Hartman et al. (2019), which contains the largest number of taxa by a factor of 2, indicates a slow–down in the rate of increase towards the present (dark blue dashed line).

82 Supertree methods provide an alternative avenue for the inference of large  
83 phylogenies of extinct taxa. Supertrees are a class of consensus tree in which a set of  
84 topologies derived from distinct datasets are summarized in some common form to yield a  
85 topology containing shared or well-supported splits (Sanderson et al. 1998; Sanderson and  
86 Driskell 2003; Bininda-Emonds et al. 2002; Bininda-Emonds, 2004). Importantly,  
87 supertree methods can accommodate sets of input trees with partially or non-overlapping  
88 leaf sets, and they therefore provide a way of synthesizing morphological character-taxon  
89 matrices covering distinct clades without re-coding characters or concatenating matrices.  
90 The best-known method for combining trees is Matrix Representation with Parsimony  
91 (MRP), where all input topologies are represented using a binary coding scheme (Fig. 2).  
92 Each column, or character, in a MRP matrix represents a bipartition from one of the  
93 source trees. An entry of “1” for a given row indicates the presence of that taxon within  
94 the clade, “0” indicates its exclusion from the clade, and “?” indicates that the taxon is  
95 not represented in the source tree in question (Baum, 1992; Ragan, 1992; Baum and  
96 Ragan, 2004, Fig 2C). A supertree containing the union of tips over the source trees may  
97 then be inferred using standard parsimony methods. Like supermatrices, supertrees (and  
98 MRP supertrees in particular) have been criticized on a number of grounds. Character  
99 non-independence necessarily arises due to reuse of characters across multiple analyses  
100 (Springer and de Jong, 2001), and issues concerning the relative quality of individual  
101 studies must also be addressed (Gatesy et al. 2004). Further sources of concern include  
102 how to select and code topologies produced from analysis of the same matrix (Gatesy  
103 et al. 2004), weighting of strongly versus weakly supported nodes (Gatesy and Springer,  
104 2004), the potential recovery of clades that are not found in any of the input trees (Pisani  
105 and Wilkinson, 2002; Bininda-Emonds, 2003; Wilkinson et al. 2005) and how best to deal  
106 with supraspecific OTUs (Page, 2004).

107 In response to these criticisms, a number of alternative supertree approaches have  
108 been developed (e.g, Bininda-Emonds, 2004; Semple et al. 2004; Levasseur and Lapointe,

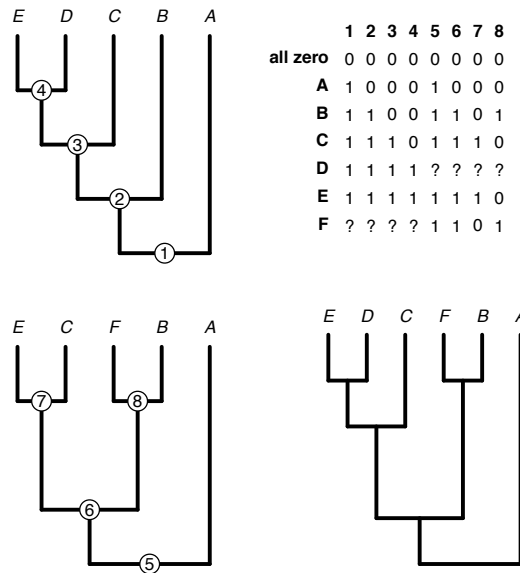


Fig. 2. Matrix representation of tree topologies allows for the inference of total clade trees even if taxa are missing from individual source trees. Here, the two source trees on the left differ in that tree 1 does not sample taxon F while tree 2 is missing taxon D. Parsimony analysis of the matrix representation of the two topologies results in a single shortest tree that captures the intuitive relationships of F with B and C as sister to D+E that are not both present in either of the two source trees.

109 [2006; Steel and Rodrigo, 2008; Lin et al., 2009; Ranwez et al., 2010; Swenson et al., 2012;  
 110 Akanni et al., 2015; Kettleborough et al., 2015; Fleischauer and Böcker 2017]). Some of  
 111 these methods allow for character weighting based on information such as bootstrap  
 112 values, or relative importance of a given source tree, but none provides a straightforward  
 113 way to explicitly accommodate phylogenetic uncertainty within individual source studies,  
 114 particularly where the number of studies is large. Furthermore, none of these approaches or  
 115 pipelines explicitly deal with earlier criticisms of the supertree paradigm that are rooted in  
 116 issues of data reuse and redundancy (Springer and de Jong, 2001; Gatesy and Springer,  
 117 2004; Gatesy et al., 2004). Lloyd et al. (2016) introduced an alternative approach that they  
 118 called a “metatree”. As with MRP supertrees, metatrees use binary encoding of tree  
 119 topologies to generate a matrix that can be analyzed using standard phylogenetic methods.  
 120 The principal difference between an MRP supertree and a metatree is that the matrix from  
 121 which MRP supertrees are built typically uses individual tree topologies gleaned from

122 published papers as data, while the metatree approach explicitly requires reanalysis of  
123 morphological character-taxon matrices to sample and encode *all* optimal topologies.  
124 Moreover, the metatree pipeline introduces specific rules to ameliorate concerns associated  
125 with data redundancy and uncertainty in the inference of source trees. In practice,  
126 metatrees tend to lead to more resolved consensus topologies than traditional MRP  
127 supertrees (compare [Lloyd et al. 2016](#) to [Lloyd et al. 2008](#)) while also better  
128 accommodating phylogenetic uncertainty in the source studies than the figured trees  
129 typically used by supertree methods ([Bell and Lloyd 2015](#)).

130 In this paper we leverage the metatree approach to assess diversification dynamics in  
131 extant and extinct cetaceans (whales, dolphins and relatives). A number of recent studies  
132 based on molecular phylogenies have provided evidence for a recent increase in cetacean  
133 net diversification rates during the past 10 Ma, driven by rapid speciation of ocean  
134 dolphins (Delphinidae) ([Steeman et al. 2009](#); [Slater et al. 2010](#); [Rabosky 2014](#); [Rabosky](#)  
135 [and Goldberg 2015](#)). However, the relative contributions of speciation and extinction rate  
136 variation to trends in net diversification can be extremely difficult to disentangle using  
137 phylogenies of extant taxa ([Liow et al. 2010](#); [Louca and Pennell 2020](#)) and the rich  
138 cetacean fossil record suggests that different dynamics may have been at play during the  
139 past 36 million years than might be suggested on the basis of molecular phylogeny alone  
140 ([Quental and Marshall 2010](#); [Morlon et al. 2011](#); [Marx and Fordyce 2015](#)). Until now, the  
141 lack of a densely-sampled higher-level phylogeny of the clade has precluded thorough  
142 comparison of diversification dynamics inferred from molecular and fossil phylogenies. We  
143 here use the metatree pipeline ([Lloyd et al. 2016](#)) to assemble a comprehensive set of  
144 phylogenetic hypotheses for extant and extinct cetaceans. We then use a Bayesian  
145 model-averaging approach (fossilBAMM [Rabosky et al. 2014](#); [Mitchell et al. 2018](#)) to  
146 estimate rates of speciation and extinction through time and across branches of the  
147 time-scaled cetacean trees. Our results demonstrate that simultaneous analysis of extinct  
148 and extant taxa can yield different conclusions regarding macroevolutionary dynamics

149 than are derived from analyses of extant taxa alone, and stress the important of  
150 paleo-phylogenetic approaches for studying macroevolutionary dynamics.

## 151 MATERIALS AND METHODS

152 The metatree approach was fully described in [Lloyd et al. \(2016\)](#) but we provide an  
153 overview here in the context of assembly of our cetacean metatree. For ease of reference,  
154 our pipeline is summarized visually as a flow-chart in [Figure 3](#) and our description of  
155 methods follow this structure.

### 156 *Data Acquisition*

157 *Morphological character data* We collected 146 morphological character matrices  
158 from 143 published studies (See Supplementary Bibliography). Sampled studies range in  
159 publication date from 1994 to 2020. New species of (typically extinct) cetacean are  
160 described with sufficient regularity that such a tree can quickly become out-of-date.  
161 However, our pipeline allows easy integration of additional data for continuous updating.  
162 We included phylogenetic analyses of exclusively extinct, exclusively extant, and both  
163 extinct and extant taxa in our dataset. The only requirement for inclusion was that a  
164 morphological character matrix was provided in the paper, the associated supplementary  
165 methods, or on some repository such as Morphobank [\(O’Leary and Kaufman 2011\)](#). All  
166 character matrices have been deposited on the cetacean metatree GitHub repository  
167 [\(<https://github.com/graemetlloyd/ProjectBlackFish>\)](https://github.com/graemetlloyd/ProjectBlackFish). We retained information  
168 regarding any character weighting or ordering schemes used in the published analyses. To  
169 minimize the impact of data duplication, we removed molecular data, where included, from  
170 each alignment.

171 *Molecular character data* Molecular evidence may provide a strong and divergent  
172 phylogenetic signal for extant taxa compared with the signal provided by morphological



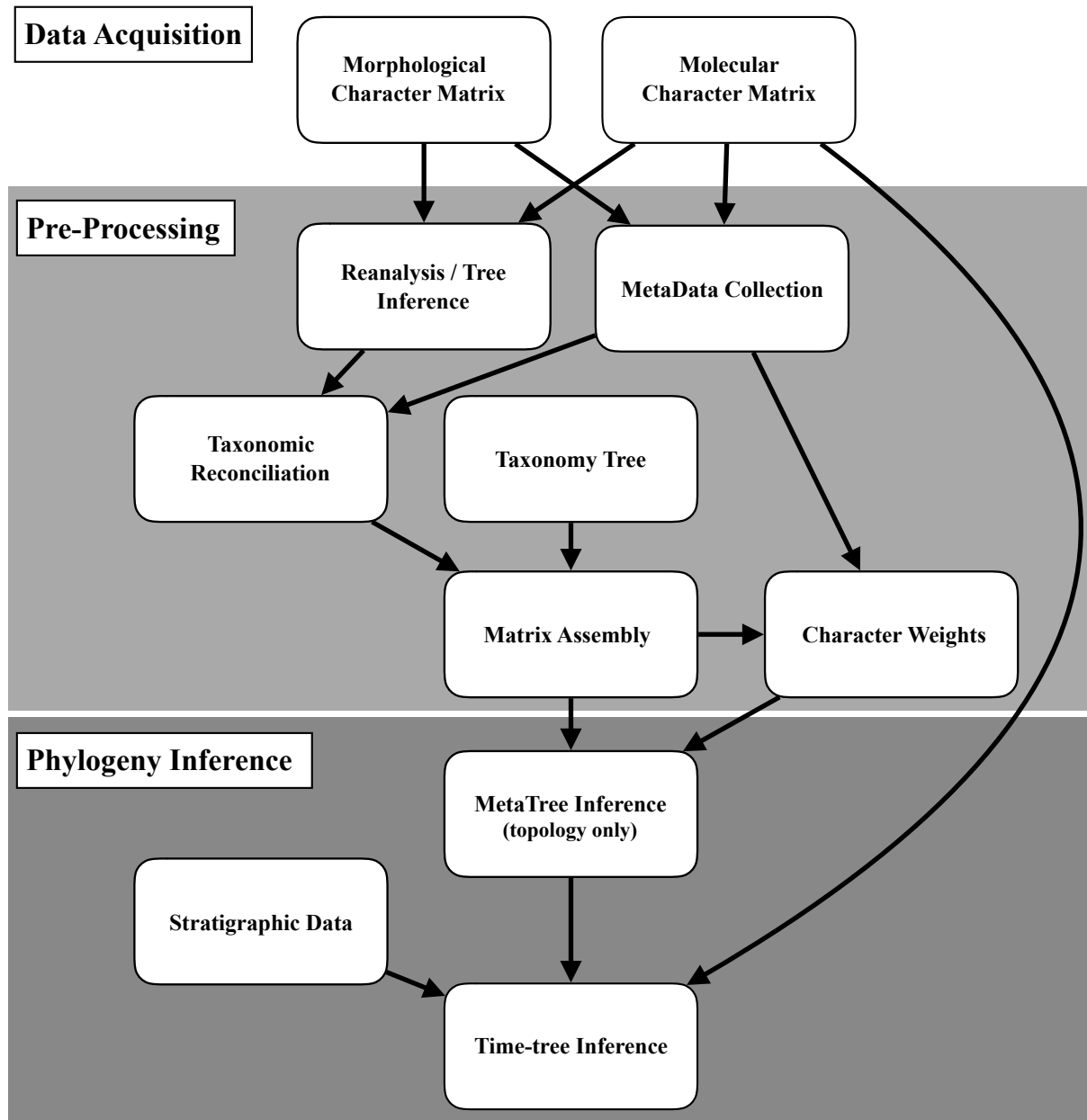


Fig. 3. Schematic showing the general outline of metatree assembly. Description of methods used in the assembly of our cetacean metatrees follow this workflow.

173 data. Parsimony analyses of morphological character data often employ a molecular  
174 scaffold approach, whereby tree searches are constrained to recover topologies for extant  
175 taxa that are consistent with molecular estimates. However, the fact that a single topology

176 constraint must typically be enforced means topological uncertainty inherent in tree  
177 inference from molecular data cannot be accommodated. The metatree pipeline can readily  
178 incorporate molecular data as an additional data source, thus accommodating topological  
179 uncertainty. We here used the molecular supermatrix of McGowen et al. (2009). This  
180 matrix contains 42,335 characters from 45 nuclear loci, mitochondrial genomes, and  
181 transposon insertion events coded for 91 taxa (four artiodactyl outgroups and 87 of 91  
182 currently recognized cetacean species).

183 *Pre-processing*

184 *Reanalysis* We reanalyzed each morphological character–taxon matrix, under the  
185 outgroup, weighting, and ordering schemes specified by the original authors, using the  
186 maximum parsimony software TNT (Goloboff et al., 2008). The use of parsimony allowed  
187 us to balance our desire to incorporate phylogenetic uncertainty via a set of most  
188 parsimonous trees with the need for an efficient pipeline for processing large numbers of  
189 source datasets while guaranteeing convergence on an optimal set of solutions. However,  
190 any approach (Maximum Likelihood, Bayesian Inference) could be used to reanalyze  
191 source data. The settings for each analysis were determined on the basis of matrix size. For  
192 24 or fewer taxa the implicit enumeration option was used, which guarantees that all  
193 optimal topologies will be returned. For 25 or more taxa, 20 separate replicates of TNT’s  
194 “New Technology Searches” were performed, each starting with a random seed. Trees from  
195 each replicate were then combined and a final round of tree bisection–reconnection was  
196 performed. In some cases the maximum tree limit (100,000) was hit, indicating additional  
197 equally optimal relationships exist. In order not to miss these topologies, searches were  
198 repeated until the least frequent bipartition was found at least twice suggesting complete  
199 coverage was reached). For the purposes of inference, trees were summarised using matrix  
200 representation, with all duplicate bipartitions removed. All unique bipartitions were  
201 equally weighted as under parsimony there is no clear basis for considering bipartition

202 frequency within the set of shortest trees as a measure of support.

203 The molecular data from McGowen et al. (2009) were analyzed in MrBayes v 3.2  
204 (Ronquist et al., 2012) via the CIPRES portal (Miller et al., 2010) using the same MCMC  
205 settings and models as in the original study. In Bayesian phylogenetic methods, topologies  
206 (and their associated branch lengths) are sampled in proportion to their posterior  
207 probabilities, which means that bipartition frequency is meaningful. We encoded unique  
208 bipartitions found within 1000 trees drawn at random from the posterior sample using  
209 matrix representation but assigned each column of the resulting character matrix a weight  
210 corresponding to its frequency in the posterior sample. For example, a clade sampled in  
211 only 10% of the posterior sample was assigned a weight that is one-tenth that of a clade  
212 present in all trees in the sample.

213 *Metadata* We recorded two key pieces of metadata from each source study. First,  
214 we noted whether supra-specific Operational Taxonomic Units (OTUs) in the character  
215 matrix were coded from a specific taxon or taxa. For example, the NEXUS file of Godfrey  
216 et al. (2017) lists the OTU *Phocageneus* but the paper itself confirms that this OTU is  
217 *Phocageneus venustus*. If a supra-specific OTU was coded from more than one taxon, all  
218 were recorded if listed in the paper. If no species-level taxa were listed, we retained the  
219 supra-specific taxon as the unit of analysis. Direct editing of names in NEXUS files can  
220 lead to problems if taxa are later synonymized or names are altered. We therefore  
221 generated custom XML files for each source study in which each OTU was reconciled to its  
222 constituent taxa, as recorded in the Paleobiology Database (Peters and McClennen, 2016).  
223 Cetaceans, both extinct and extant, are extremely well documented in the Paleobiology  
224 Database thanks largely to the efforts of Mark Uhen (e.g., Uhen and Pyenson, 2007).  
225 Additionally, as the database is continually updated and has an API (Peters and  
226 McClennen, 2016), dynamic updating of taxonomy can be achieved in future metatree  
227 iterations. Seventy undescribed OTUs did not have a species name. Following Lloyd et al.  
228 (2016) we retain these as “valid” taxa in our analyses because 1) they may represent key

229 data for resolving phylogenetic relationships, dating the tree, or performing downstream  
230 macroevolutionary analysis, and 2) there is a clear and repeated tendency for these  
231 specimens to become the holotypes of new species (for example, the specimen-level OTU,  
232 “GSM 109” was included in multiple trees prior to its formal description as *Echovenator*  
233 *sandersi* by Churchill et al. (2016). Such OTUs are a common feature in other clades too;  
234 10% (97 of 961) of OTUs in Lloyd et al. (2016) were unnamed specimens.

235 The second piece of information noted was whether the matrix was based on a  
236 previous study. For example, the matrix of Godfrey et al. (2017) was based on an earlier  
237 study by Lambert et al. (2014) and was itself later used by Boersma et al. (2017). This  
238 information was added to each matrix’s XML file for use in determining relative weighting  
239 or study redundancy when assembling the final MRP matrix.

240 *Taxonomic reconciliation and taxonomy tree* Before matrix representations for  
241 each source study can be combined to form a global matrix, a list of valid species must be  
242 decided on and taxonomic assignments reconciled to this list. We dynamically reconciled  
243 tip names recorded in the XML files to currently valid taxon names recognized in the  
244 Paleobiology Database, for example updating junior synonyms to their senior synonyms.  
245 This procedure allows taxonomic information to be automatically updated and limits  
246 human error while updating names.

247 The taxonomic hierarchy present in the database also represents a  
248 pseudo-phylogenetic hypothesis (Soul and Friedman, 2015), a feature exploited here in two  
249 ways. First, supraspecific taxon rows that cannot be reconciled to specific taxa can be  
250 replaced with a set of duplicated rows corresponding to species-level OTUs, avoiding the  
251 situation where, for example, *Balaenoptera* and *Balaenoptera musculus* exist as separate  
252 tips in the final metatree. Second, the taxonomy can be included as an additional, albeit a  
253 heavily down-weighted data set (Gatesy and Springer, 2004). This is important as the  
254 presence of a basic but comprehensive estimate of phylogeny derived from taxonomy can  
255 ameliorate inference issues that might arise due to a lack of data overlap (an affliction of

256 formal supertrees often termed “rogue taxa”). For example, Mysticetes and Odontocetes  
257 should logically be separated as clades, but if all phylogenetic analyses only focused on one  
258 or the other of these clades, then information on their reciprocal monophyly would be  
259 lacking.

260 The use of a taxonomy tree also allows for the inclusion of species that are  
261 un-sampled in the set of source trees. Higher-level analyses of extant clades have included  
262 taxa for which molecular data are unavailable by simultaneously enforcing topology  
263 constraints, based on taxonomy, and integrating over possible placements of missing taxa  
264 under a birth–death process (e.g., [Kuhn et al. 2011](#); [Jetz et al. 2012](#); [Rabosky et al. 2018](#);  
265 [Upham et al. 2019](#)). We here increased taxonomic coverage for fossil cetaceans by  
266 producing two additional versions of our MRP matrix, one in which all species assigned to  
267 a sampled genus were included and another where all species assigned to Cetacea in the  
268 Paleobiology Database were included. We refer to these analyses as GENUS and ALL,  
269 respectively, for the remainder of this paper, with the species-level analysis referred to as  
270 EXCLUDE to account for the fact that unsampled OTUs were excluded. It should be  
271 stressed that, because our pipeline treats taxonomic bipartitions as data that are  
272 down-weighted relative to bipartitions derived from phylogenetic analyses, this approach  
273 does not force a taxonomic structure on the result where there are primary character data  
274 available that disagree with it (cf. [Jetz et al. 2012](#); [Rabosky et al. 2018](#); [Upham et al.](#)  
275 [2019](#)).

276 *Matrix assembly and character weighting* After taxonomic reconciliation, it is  
277 straightforward to merge MRP matrices from source studies into a global character–taxon  
278 matrix. At this stage, we also compute character weights, based on three attributes of  
279 source studies: non-independence, date of publication, and size (measured in number of  
280 MRP characters). Older character matrices that were reused in a subsequent study without  
281 modification of the characters themselves (e.g., by the addition of a single new taxon to an  
282 existing dataset) were deemed redundant and automatically removed. The remaining

283 non-independent data sets were assigned equal weights that sum to one, with this weight  
284 being applied to each character of the data set. Next, following [Lloyd et al. \(2016\)](#),  
285 publication year weights were assigned such that the oldest included data-set received a  
286 weight of 10 (an order of magnitude higher than the weight assigned to the taxonomy tree)  
287 and with weights doubling every two years. Again, this weight was applied to each  
288 character in a data set. Finally, some data sets generated more MRP characters than others  
289 simply because they contained greater phylogenetic uncertainty and without intervention  
290 these would dominate the final tree. To account for this individual characters (bipartitions)  
291 were weighted such that any within-data-set characters (bipartitions) with which they  
292 conflict are clustered and down-weighted such that they sum to one, with any unconflicted  
293 characters being weighted one. These different character weights were combined by taking  
294 the product of the three criteria-based weights. Other ways of weighting characters and  
295 source studies are possible (interested readers can consult the *in development metatree* R  
296 package [github.com/graemetlloyd/metatree](https://github.com/graemetlloyd/metatree) for more information and options) but we  
297 have so far found the above to work well across a range of groups.

298 TNT ([Goloboff et al. 2008](#)) requires that weights fall in the range 0.50 – 1000.00.  
299 We set default weights of one for the taxonomy tree (always enforced) and 10 for the  
300 minimum phylogenetic weight, but no initial maximum weight can be specified and in  
301 practice this may exceed 1000.00. When this occurred, we rescaled the phylogenetic  
302 weights only to fall on a 10.00 – 1000.00 scale. [Lloyd et al. \(2016\)](#) applied multistate  
303 characters to effectively stretch this maximum possible weight to 31000.00, but we found  
304 that this dramatically slowed the run time of TNT. Thus when it came time to upweight  
305 molecular topologies relative to morphological topologies, we instead assigned them  
306 maximum weights combined with column (character) duplication. Column duplication is  
307 identical to numerically upweighting character state changes or site likelihoods using  
308 integer-valued weights, and is the method employed in model-based phylogenetic inference  
309 tools such as RAxML ([Stamatakis, 2014](#)) and BEAST 2 ([Bouckaert et al. 2014](#)).

*Phylogeny Inference*

310

311 *Metatree inference* Prior to analysis, the final MRP matrix was subjected to Safe  
312 Taxonomic Reduction (STR: [Wilkinson, 1995](#)) using the `SafeTaxonomicReduction()`  
313 function in the R ([R Development Core Team, 2019](#)) package `Claddis` ([Lloyd, 2016](#)) and  
314 an all-zero outgroup was added to provide character polarity during the tree search  
315 ([Baum, 1992](#); [Ragan, 1992](#)). We performed 1000 independent parallel tree searches using  
316 TNT with the `xmult` option for multiple replications using sectorial searches, drifting,  
317 ratchet and fusing invoked at level 10, and a maximum of 1000 trees held in memory  
318 ([Goloboff et al., 2008](#)). We reinserted STR taxa using the `SafeTaxonomicReinsertion`  
319 function in `Claddis` ([Lloyd, 2016](#)) and constructed a strict consensus tree from the final  
320 sample of shortest trees.

321

*Time-tree Inference* The result of metatree inference is a set of most parsimonious  
322 topologies that can be summarized using consensus methods. However, macroevolutionary  
323 analyses require topologies with associated branch lengths in units of time. Paleontological  
324 approaches for time scaling phylogenies have historically been somewhat arbitrary in  
325 nature (for a review see [Hunt and Slater, 2016](#)). However, these approaches have recently  
326 been superseded by probabilistic methods that allow for simultaneous inference of topology  
327 and branch lengths for extinct and extant species under a birth-death process ([Heath](#)  
328 [et al., 2014](#); [Gavryushkina et al., 2014, 2017](#)).

329

We combined three sources of data to sample a distribution of time-scaled  
330 phylogenies for extinct and extant cetaceans using BEAST 2.5.2 ([Bouckaert et al., 2014](#)).  
331 We first used the strict consensus metatree topology to derive a series of topological  
332 constraints for each BEAST analysis. No character data were used for extinct taxa and so  
333 no morphological clock was invoked to derive branch lengths. In an analysis of extant taxa  
334 only, the resulting topological arrangements among unconstrained taxa would be random,  
335 but for extinct taxa they are influenced by stratigraphic age, via the use of the Fossilized

336 birth–death process tree prior (Heath et al., 2014; Gavryushkina et al., 2014, 2017). As a  
337 result, sampled topologies can be thought of as reflecting a balance between strong prior  
338 belief, in the form of hard topological constraints derived from metatree inference, and  
339 stratigraphic data. For each extinct terminal taxon in our strict consensus topology, we first  
340 queried the Paleobiology Database to obtain the age of first occurrence. The age of each  
341 taxon was then specified as the beginning and end dates for the stage of first occurrence,  
342 based on the 2018 International Commission on Stratigraphy updated chronostratigraphic  
343 chart (<http://stratigraphy.org/ICSchart/ChronostratChart2018-07.pdf>). Where  
344 possible, we supplanted PBDB–derived ages, with more refined biostratigraphic or  
345 radiometric age estimates taken from primary sources or previous phylogenetic analyses  
346 and revisions (Table S1).

347 We selected a subset of the alignment from McGowen et al. (2009) for use in our  
348 BEAST analyses. Molecular data can provide important information regarding the relative  
349 branch lengths for extant taxa, particularly in clades lacking fossil representatives.  
350 Preliminary attempts to perform BEAST analyses using the entire alignment yielded poor  
351 mixing, even after very long ( $> 10^8$  generations) runs. We therefore used SortaDate (Smith  
352 et al., 2018) to identify and rank genes that were most congruent with the topology  
353 reported by McGowen et al. (2009) and that displayed the most clock–like behavior. Based  
354 on these criteria *Cytochrome B* was identified as the most appropriate gene and was used  
355 in Bayesian estimation of topology and branch lengths (note that the same gene was used,  
356 due to its availability for all 87 extant taxa, in McGowen et al. (2009)). We determined that  
357 an uncorrelated relaxed clock with log–normally distributed rates best fitted the molecular  
358 data, based on comparison of marginal likelihoods computed for a fixed topology of extant  
359 taxa (see Supplementary Information). We set informative priors on the net diversification  
360 ( $r \sim \text{exponential}[1.0]$ ), and relative extinction rates ( $\epsilon \sim \beta[2.0, 1.0]$  based on Marshall’s  
361 2017 third paleobiological law that speciation  $\approx$  extinction), and placed a flat prior on  
362 fossilization probability ( $s \sim U[0, 1]$ ). For the origin of the FBD process we specified an



363 offset exponential prior, with an offset of 54 million years, corresponding to the age of the  
364 oldest known cetacean *Himalayacetus subanthuensis* (Bajpai and Gingerich, 1998), and  
365 mean of 3.5 that resulted in a 95% quantile corresponding to the Cretaceous – Paleogene  
366 boundary (66 Ma). We ran two chains for  $10^8$  generations, sampling every  $10^5$  generations  
367 and, after visually checking for convergence and parameter effective sample sizes  $> 200$   
368 using Tracer v1.7.1, we discarded a chain-specific burn-in and combined tree files.  
369 Attempts to produce a maximum clade credibility tree annotated with mean or median  
370 branch lengths failed due to negative branch lengths, indicating conflict between the most  
371 frequently sampled topology and the distribution of underlying branch lengths. Instead, we  
372 sampled the Maximum *A Posteriori* (MAP) tree for visualization purposes and for  
373 subsequent macroevolutionary analysis.

#### 374 *Inference of Diversification Dynamics*

375 Analyses based on molecular phylogenies of extant cetacean phylogeny have  
376 recovered evidence for an increase in mean net diversification rates during the past 10 Ma,  
377 driven by increased rates of speciation in oceanic dolphins (McGowen et al., 2009; Steeman  
378 et al., 2009; Slater et al., 2010; Rabosky et al., 2014). It is well known that inference of  
379 trait evolution dynamics can be misleading when based on phylogenies of extant taxa alone  
380 (Finarelli and Flynn, 2006; Slater et al., 2012, 2017) and some evidence suggests that  
381 inference of cetacean diversification dynamics may suffer from similar issues (Quental and  
382 Marshall, 2010; Morlon et al., 2011). We used fossilBAMM (Mitchell et al., 2018) to infer  
383 speciation and extinction dynamics for each of the MAP time-scaled cetacean metatrees.  
384 As with the standard form of BAMM (Rabosky et al., 2014), fossilBAMM is a Bayesian  
385 model-averaging approach that samples speciation and extinction rates along branches of  
386 a phylogenetic tree while allowing for shifts in one or both rates. The method requires a  
387 bifurcating, time-scaled tree containing living and extinct taxa, as well as the number of  
388 unique fossil occurrences for tips included in the tree. We queried the Paleobiology

389 Database to recover unique stratigraphic occurrences associated with each terminal taxon  
390 present in each of the three metatrees. Taxa not in the database (i.e., undescribed taxa)  
391 were treated as having unique single occurrences. Prior to analysis, we also pruned  
392 sampled ancestors from the MAP trees to avoid biasing estimates of speciation and  
393 extinction due to very short terminal edges. We determined priors for each analysis by  
394 using the `setBAMMpriors` function in the `BAMMtools` library (Rabosky et al., 2014) and ran  
395 two independent MCMC chains for  $10^8$  generations, sampling every  $10^4$ . We checked for  
396 convergence and large effective sample sizes using functions in the `coda` library (Plummer  
397 et al., 2006) and processed post-burnin output using functions from the `BAMMtools` library  
398 (Rabosky et al., 2014). To compare and contrast trends in diversification dynamics derived  
399 from the three metatrees, we plotted median and 95% confidence intervals for speciation,  
400 extinction and net diversification rates through time using the `plotRateThroughTime()`  
401 function. To compare branch and clade specific rates, we also plotted mean per-branch  
402 rates on the respective phylogenetic hypotheses.

## 403 RESULTS

### 404 *Metatree Inference*

405 Analysis of the 147 source studies (146 morphological plus 1 molecular) resulted in  
406 an MRP matrix comprising 494 species, approximately two-thirds of all recognized  
407 cetacean taxa, and 14257 binary characters. Safe Taxonomic Reduction reduced the size of  
408 the matrix for analysis to 440 taxa. The strict consensus of 1000 most parsimonious trees,  
409 after reinsertion of STR tips, is remarkably well-resolved (78% of nodes, Fig 4a) with  
410 polytomies concentrated in basilosaurid archaeocetes, Balaenopteroidea (including extant  
411 rorquals), squalodontid odontocetes, and the beaked whale genus *Mesoplodon*. Adding taxa  
412 to the taxonomy source tree allowed us to increase taxonomic coverage but, without  
413 additional data to place the new species, tended to lead to much less well resolved strict

414 consensus topologies. Specifically, the percentage of resolved nodes dropped to 56% in the  
415 GENUS tree (615 taxa, 14326 characters; Fig 4b) and to 29% for the ALL tree (746 taxa,  
416 14344 characters; Fig 4c).

417 The lack of resolution in the ALL strict consensus metatree, in particular, poses  
418 problems for reliable inference of topology and branch lengths during time–tree inference.  
419 We therefore used Matrix Representation with Likelihood (MRL; Nguyen et al., 2012) to  
420 generate a more stable estimate of topology for this dataset. We first switched the codings  
421 of 50% of data columns selected at random, such that “0” became “1” and vice versa to  
422 avoid violating the assumptions of the symmetric Markov models employed in  
423 phylogenetics software. We then used RAxML v. 8 (Stamatakis, 2014) to find the  
424 maximum likelihood estimate of topology under the BINCAT model with rate  
425 heterogeneity disabled (–V option). Taxa removed during safe taxonomic reduction were  
426 subsequently reinserted and the resulting tree was then used as a topology constraint for  
427 BEAST analyses.

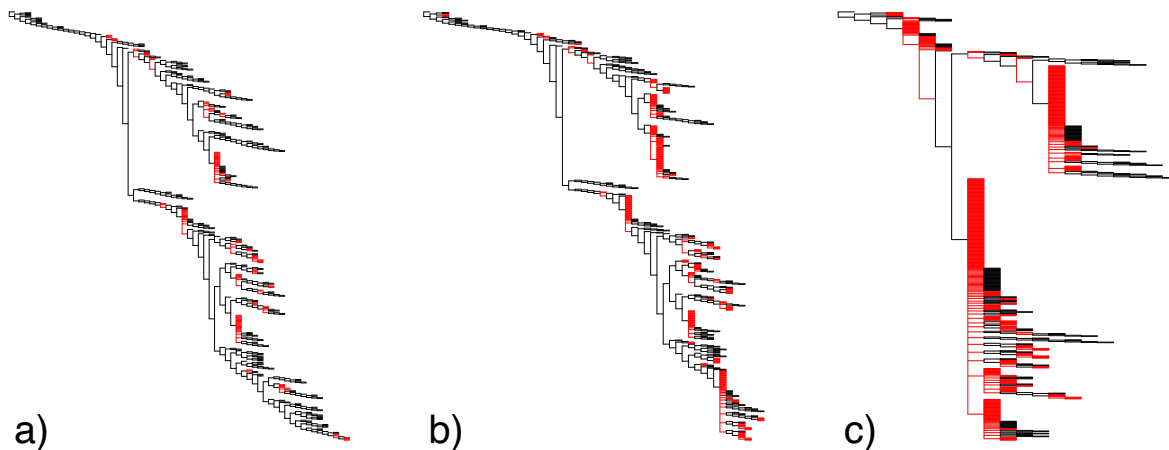


Fig. 4. Strict Consensus metatrees of cetaceans based on inclusion of a) 494 species–level OTUs from source trees, b) 615 species belonging to genus–level OTUs from source trees, and c) all 746 valid cetacean taxa recorded in the Paleobiology Database. Black edges represent those branches arising from bifurcating nodes. Red edges are those arising from polytomies either due to uncertainty in the MPT set or due to reinsertion of taxa that were removed prior to analysis during safe taxonomic reduction.

*Time-tree Inference*

428

429 The availability of stage-level or finer stratigraphic data reduced the number of  
430 taxa from 494 to 487 for Bayesian estimation of topology and branch lengths for the  
431 EXCLUDE dataset. Divergence time estimates among extant clades in the MAP tree (Fig  
432 5) are broadly consistent with previously published estimates for cetaceans but the  
433 inclusion of extinct taxa yields novel insights into the timescale of whale evolution. The  
434 cetacean stem extends back to 51.3 Ma, with the divergence of the semi-aquatic  
435 archaeocete clade Pakicetidae (*Pakicetus*, *Ichthyolestes*, and *Nalacetus*) from all other  
436 cetaceans. Fully aquatic cetaceans (the Pelagiceti of Uhen, 2008) originate at 41.7 Ma with  
437 the divergence of a clade comprising the paraphyletic Basilosauridae and Neoceti. The  
438 time-scaled metatree emphasizes that many of the gaps along long internal branches of  
439 molecular time-trees should be filled with now-extinct radiations. For example, the long  
440 stem lineage leading to crown odontocetes that is implied by molecular phylogenies is filled  
441 in by the radiations of Xenorophidae, Waipatiidae, Patricetidae, and Squalodontidae. The  
442 former diversity of Physeteroidea and Platanistoidea is also apparent in the time-scaled  
443 tree, despite the low diversity of these clades in modern times (3 and 1 extant species,  
444 respectively).

445 Bayesian estimation of branch lengths on the GENUS and ALL datasets resulted in  
446 larger time trees with more fossil taxa but yielded substantially older divergence times for  
447 some crown clades than we found for the EXCLUDE dataset. To facilitate comparison of  
448 our results to divergence time estimates derived from node-dated trees, we extracted mean  
449 ages and their associated 95% HPD intervals for select crown clades and compared them to  
450 those inferred by McGowen et al. (2019) using a genomic dataset. These estimates (Table  
451 1) show that node age estimates are relatively consistent between the genomic tree and our  
452 EXCLUDE metatree, albeit with the metatree generating slightly younger node ages. Node  
453 ages for the GENUS and ALL datasets are, on average, a little older than those in the  
454 EXCLUDE tree and more similar to those of the genomic tree. Balaenidae and

CETACEAN METATREE AND DIVERSIFICATION

21

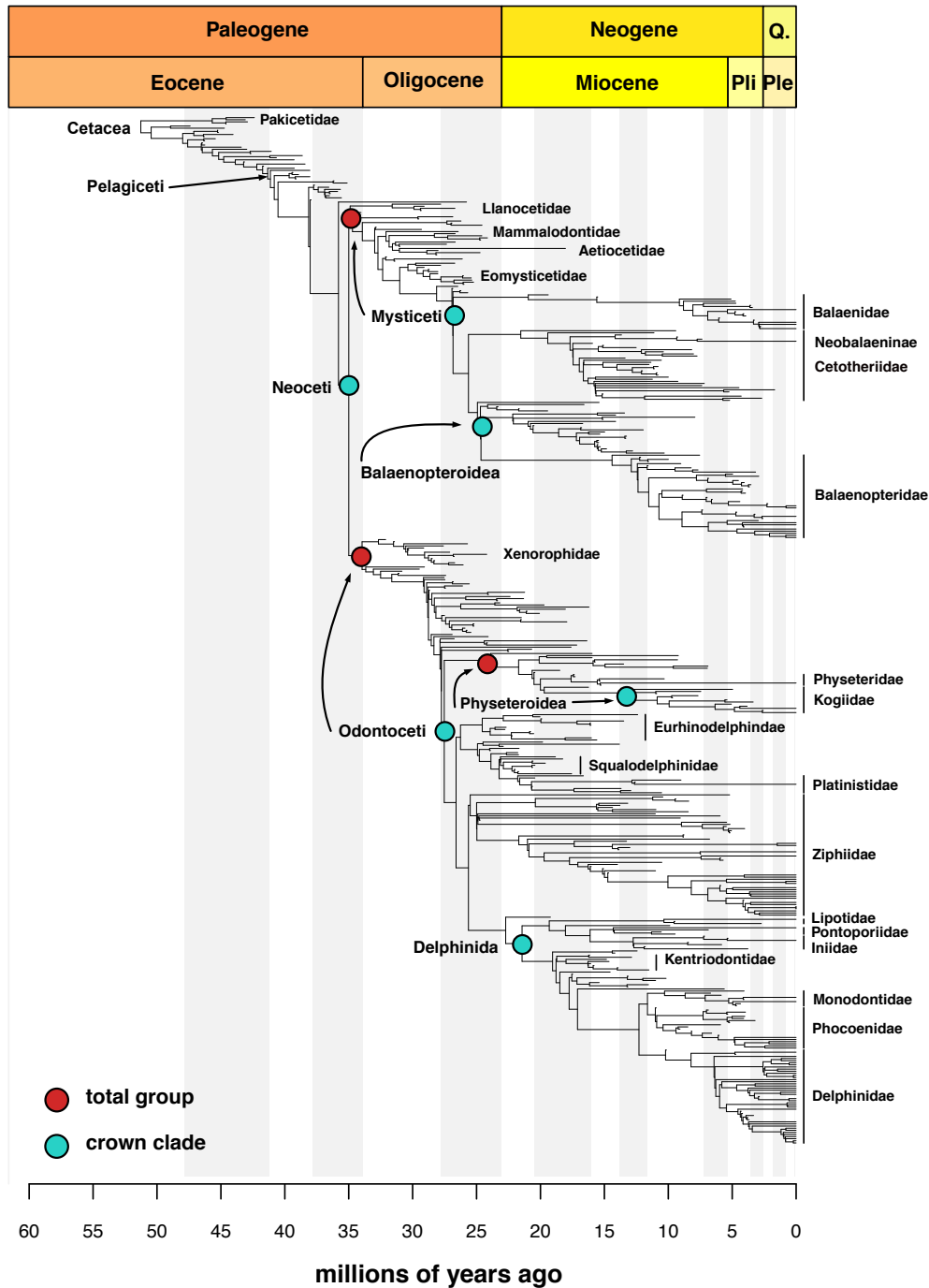


Fig. 5. Maximum *a posteriori* chronogram derived from simultaneous Bayesian inference of topology and branch lengths. The strict consensus metatree derived from analysis of species-level OTUs is used as a topology constraint with stratigraphic ages for extinct taxa and *Cytochrome B* sequence data for extant taxa used to help resolve polytomies. Shaded bars correspond to marine stages.

455 Delphinidae deviate substantially from this pattern, however, with mean age estimates  
456 that are approximately 10 and 7 million years older, respectively, than the EXCLUDE  
457 dataset and have 95% HPD intervals that do not overlap.

Table 1. Divergence time estimates (mean and 95% HPD intervals) for select crown clades from the genomic study of McGowen et al. (2019) and the three metatree analysis.

Clade	McGowan et al. (2019)	EXCLUDE	GENUS	ALL
Neoceti	36.7 (37.5–36.4)	36.8 (38.4–35.2)	37.8 (39.3–35.4)	40.3 (42.0–38.3)
Mysticeti	25.7 (26.7–25.2)	23.3 (28.1–24.4)	26.8 (28.4–24.5)	28.7 (31.2–26.4)
Balaenidae	10.6 (12.1–9.2)	6.9 (8.3–5.9)	17.2 (18.4–15.5)	17.8 (19.6–16.0)
Balaenopteridae	15.7 (16.9 – 14.7)	13.0 (16.2–9.7)	15.9 (18.5–12.3)	20.5 (22.4–18.4)
Odontoceti	34.1 (34.9–33.7)	28.0 (26.7–29.5)	28.6 (29.7–26.8)	31.9 (33.5–30.2)
Physteroidea	22.4(24.1–20.6)	21.0 (23.2–18.4)	23.1 (24.5–21.2)	25.0 (27.7–22.4)
Delphinida	25.1 (26.1–24.2)	21.4 (23.7–19.2)	22.9 (25.1–20.3)	23.2 (25.1–21.4)
Delphinidae	12.7 (13.6–11.8)	8.7 (10.6–6.7)	15.7 (16.7–13.8)	17.4 (19.7–15.4)

### 458 *Inference of Diversification Dynamics*

459 Similar to analyses based on extant cetaceans alone, we found that net  
460 diversification rates are relatively constant through time, but with a rapid increase in mean  
461 net diversification rates beginning at approximately 10 Ma for the EXCLUDE MAP  
462 chronogram. In contrast with inference from molecular phylogenies, this result arises not  
463 only from a moderate increase in speciation rates, but also from a precipitous decline in  
464 extinction rates over the same time frame (Figs 6 b,c). These average rates are clearly  
465 emergent properties of more complex, clade-specific dynamics. The 95% credible shift set  
466 for the EXCLUDE MAP tree contained 483 distinct configurations, with 2 – 6 shifts  
467 recovered most often (Table 2). No individual configuration occurred with any meaningful  
468 frequency ( $f = 0.055$  or less). However, plots of mean per-branch speciation, extinction,  
469 and net diversification rates show that elevated net diversification rates in mesoplodont  
470 beaked whales, a result not previously identified in molecular phylogenies, result from  
471 depressed rates of extinction against a backdrop of already low rates of speciation, while  
472 rapid diversification rates in oceanic dolphins result from both elevated speciation and  
473 depressed extinction rates (Figs 7 a-c).

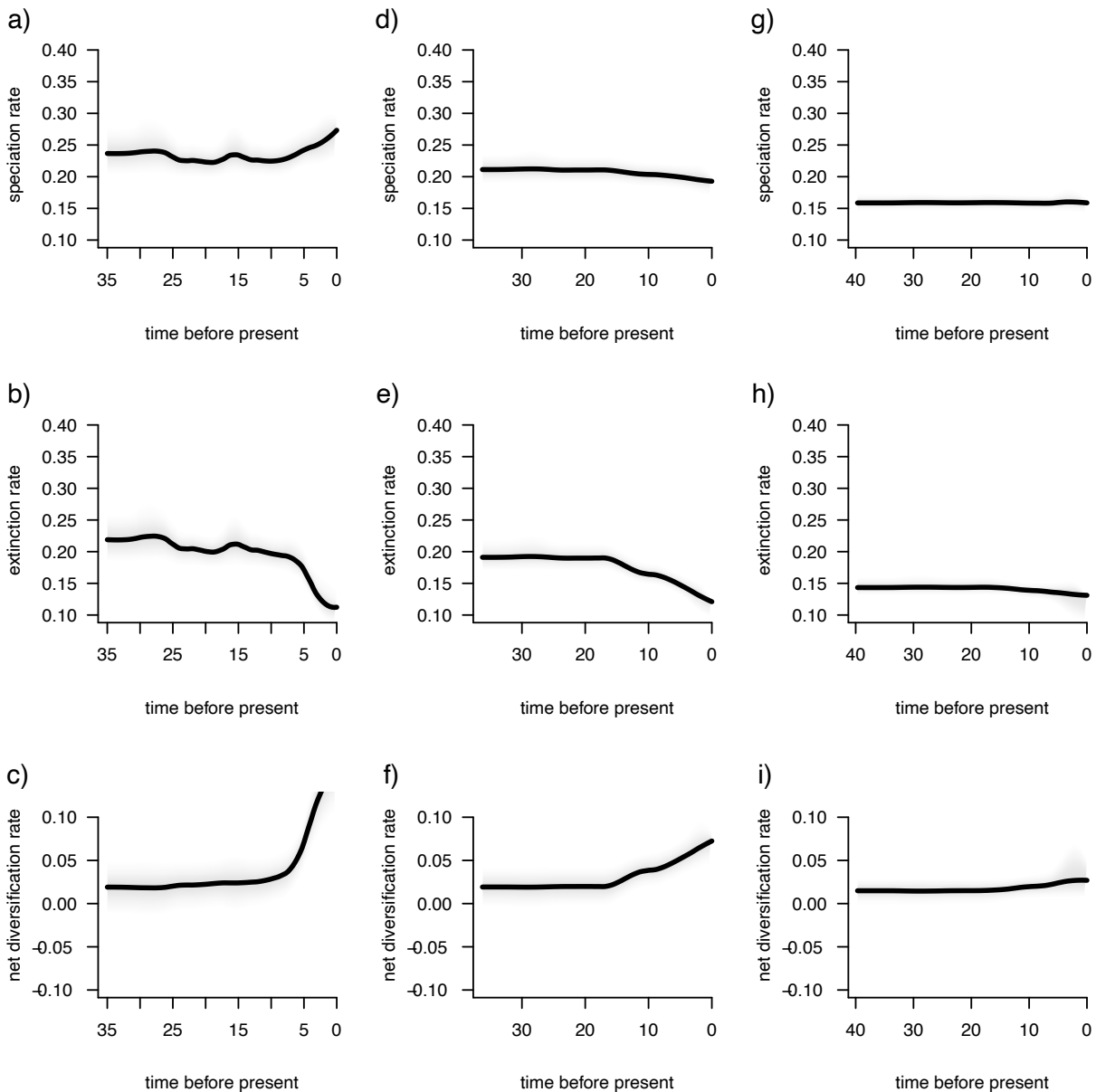


Fig. 6. Diversification dynamics through time inferred from the EXCLUDE (a:c), GENUS (d:f), and ALL (g:i) datasets suggest very different dynamics through time. Note that Speciation and Extinction rates are plotted on the same scale as each other, and as in [Rabosky 2014](#) figure 9D:E) for extant cetaceans.

474

Increases in mean net diversification rates towards the present day are more muted

475

in the GENUS chronogram (Figs [6](#) d-f). Although we recovered similarly declining mean

476

extinction rates as for the EXCLUDE tree, we found no increase in mean speciation rates

477

and, in fact, recovered a slight decline over this time-frame (Figs [6](#) d,e). The number of

Table 2. Posterior probabilities for numbers of rate shifts (N. shifts) on the 3 MAP time-scaled metatrees.

N.Shifts	Exclude	Genus	All
0	0	<0.01	0.46
1	<0.01	0.51	0.23
2	0.14	0.36	0.18
3	0.29	0.09	0.10
4	0.23	0.02	0.02
5	0.17	<0.01	<0.01
6	0.11	0	<0.01
7	0.03	0	0
8	0.02	0	0
9	<0.01	0	0
10	0	0	0
11	<0.01	0	0

478 inferred shifts is much lower for the GENUS dataset (Table 2), and only 83 possible  
479 configurations are present in the 95% credible set. Mean per-branch rates (Figs 7d-f) show  
480 that the more muted increases in net diversification for mesoplodontid ziphiids and ocean  
481 dolphins arise from decreased extinction rates in these clades.

482 Rate variation is further dampened in the ALL analysis. Here, there is no increase  
483 in mean net diversification rate and both mean speciation and extinction rates have  
484 remained relatively low and constant, albeit with a very slight increase in speciation and  
485 decline in extinction at approximately 10 Ma (Figs. 6g-i). Although a configuration with  
486 no shifts was the most frequently sampled (Table 2), 154 alternative configurations are  
487 present in the 95% credible set. Mean per-branch rates of speciation and extinction are  
488 relatively homogeneous, but with very slight increases in speciation and decreases in  
489 extinction rates, leading to slight increases in net diversification in delphinids (Figs. 7g:i).

## 490 DISCUSSION

491 The ability to infer comprehensively sampled phylogenies of extant higher-level  
492 clades has led to novel hypotheses regarding their macroevolutionary dynamics (Smith  
493 et al., 2009; Smith and Brown, 2018; Jetz et al., 2012; Zanne et al., 2014; Cooney et al.,  
494 2017; Tonini et al., 2016; Jetz and Pyron, 2018; Rabosky et al., 2018; Upham et al., 2019;  
495 Varga et al., 2019). However, even a limited amount of data from fossil taxa can overturn



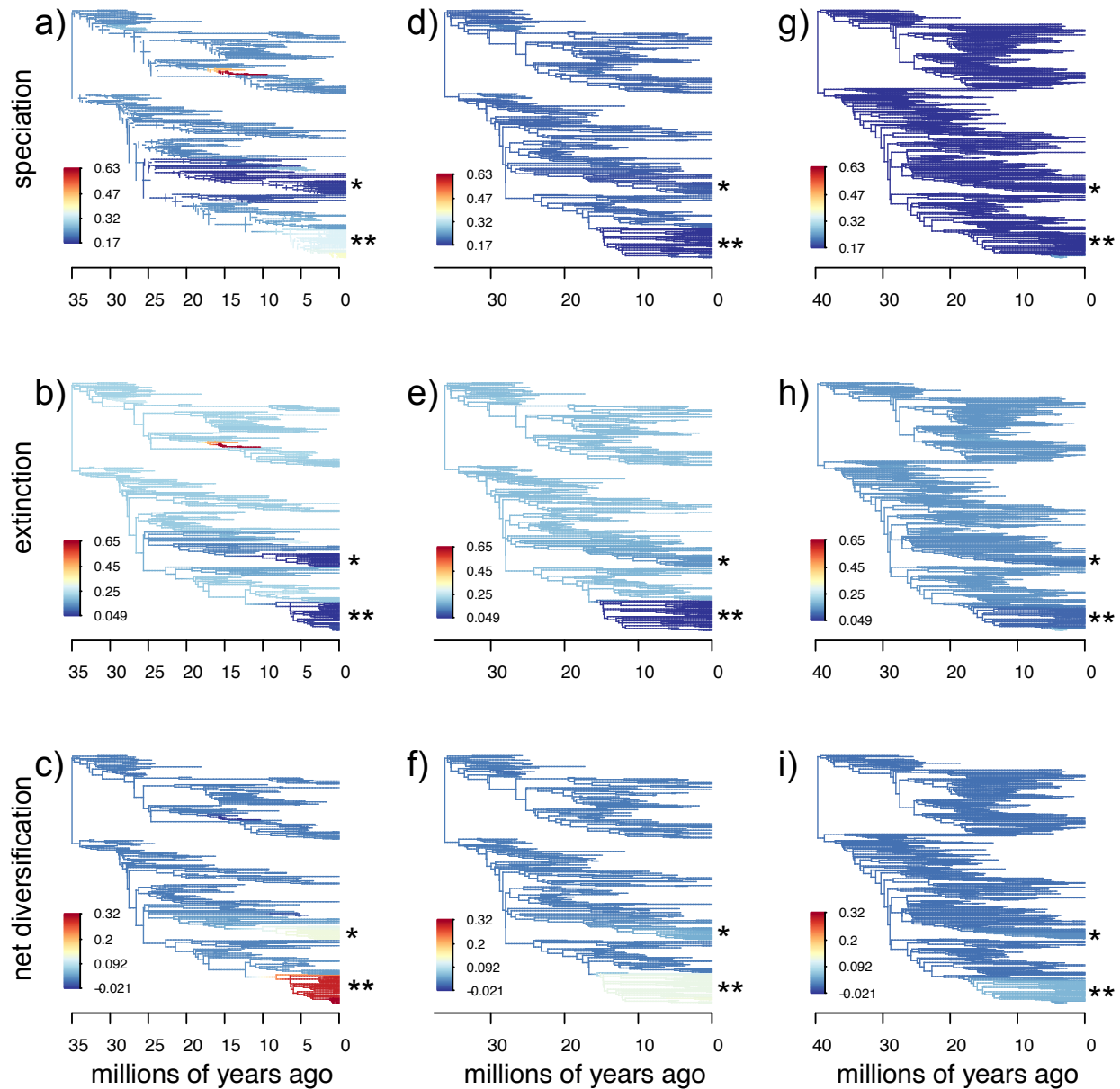


Fig. 7. Mean per-branch rates of speciation, extinction, and net-diversification rates for the EXCLUDE (a:c), GENUS (d:f), and ALL (g:i) datasets. As in Figure 6 the top row is speciation rates, middle row is extinction rates, and bottom row is net diversification rate. The single asterisk (\*) denotes mesoplodont beaked whales, the double asterices (\*\*) denote oceanic dolphins (Delphinidae). Note that the same scale is used for each plot to enable comparisons of absolute magnitudes of the underlying estimated rates.

496 well-supported hypotheses derived from analyses of extant taxa only (Finarelli and Flynn  
497 2006; Albert et al. 2009; Slater et al. 2012; Betancur-R et al. 2015; Meseguer et al. 2014)  
498 and it is likely that datasets consisting exclusively or primarily of fossil taxa are needed to

499 test fundamental macroevolutionary hypotheses. The most substantial barrier to  
500 implementing such tests has always been the difficulty in assembling robust, time-scaled  
501 phylogenies for higher-level clades that contain sufficient numbers of fossil taxa. Our  
502 well-resolved cetacean metatrees suggests that meta-analytic phylogenies can provide a  
503 useful and compelling way of synthesizing studies of lower-level clades to produce  
504 higher-level phylogenetic hypotheses for extinct taxa. Moreover, these trees provide an  
505 accessible way of addressing questions of macroevolutionary importance using fossil data  
506 and allow for the interrogation of results derived from phylogenies of extant taxa alone.

### 507 *Implications for Cetacean Diversification*

508 It has been recognized for some time that estimates of extinction rates derived from  
509 molecular phylogenies may be problematic (Rabosky, 2010; Beaulieu and O'Meara, 2015).  
510 Empirical studies have found that diversification rates estimated from molecular  
511 phylogenies may be congruent with inferences derived from paleontological data but often  
512 differ in the underlying estimates of speciation and extinction rates over time (e.g.,  
513 Simpson et al., 2011; Cantalapiedra et al., 2015; Hagen et al., 2017; Law et al., 2017). The  
514 myriad ways in which speciation and extinction rates can vary to produce identical lineage  
515 through time plots for phylogenies of extant species was recently emphasized by Louca and  
516 Pennell (2020). One of the many implications of their work is that the dimensionality of  
517 model space (that is, the number of possible combinations of time-varying speciation and  
518 extinction rates) is too large to reliably identify the generating model when only extant  
519 species are sampled and that robust inference of speciation and extinction rates through  
520 time can only be achieved with densely sampled phylogenies that incorporate extinct and  
521 extant lineages.

522 One of the most striking results to emerge from our diversification analyses is that  
523 variation in extinction rates, rather than speciation rates, have played a dominant role in  
524 shaping extant cetacean diversity. It is, of course, a mathematical necessity that rates of

525 speciation must increase or rates of extinction decline in order for net diversification rates  
526 to increase. But, while many neontologists have (explicitly or implicitly) assumed a  
527 dominant role for elevated rates of speciation in driving diversification in exceptionally  
528 species-rich clades as a response to increased ecological opportunity (for reviews, see  
529 Schluter, 2000; Glor, 2010; Stroud and Losos, 2016; Martin and Richards, 2019),  
530 paleontologists have tended to recognize a role for extinction rate variation in facilitating  
531 radiations over geologic time-scales (Jablonski et al., 1983; Van Valen, 1985; Labandeira  
532 and Sepkoski, 1993; Valentine, 1990). However, the difficulty of inferring extinction from  
533 molecular phylogenies means that the effects of extinction rate variation have received  
534 little attention in phylogenetic contexts. Here, by incorporating fossil taxa in a  
535 phylogenetic framework, we found that mesoplodont beaked whales emerge as a previously  
536 unidentified rapid radiation. Despite accounting for 15 of 21 extant species (Mead and  
537 Brownell Jr (1993), this radiation is not characterized by elevated speciation rates but,  
538 rather, by depressed extinction (Fig. 7b). Fossil evidence from diverse taxa has showed  
539 that clade-level origination and extinction rates tend to be positively correlated (Stanley,  
540 1979), meaning that clades with a higher instantaneous probability of speciating tend to  
541 also have a higher long-term probability of going extinct (higher volatility: Gilinsky, 1994),  
542 while clades with low extinction probabilities are more extinction resistant (Valentine,  
543 1990). Recent work has found a strong link between ecological diversity and low volatility  
544 across living and extinct clades of marine animals (Knope et al., 2020), suggesting that low  
545 extinction at the clade level may arise due to factors such as ecological flexibility.  
546 Unfortunately, too little is currently known about mesoplodont ecology to derive  
547 reasonable hypotheses to explain their low extinction rates and macroevolutionary success.

548 Diversification studies based on extant cetacean phylogenies have consistently  
549 identified the oceanic dolphins as a rapid radiation due to elevated speciation rates during  
550 the past 10 myr (McGowen et al., 2009; Steeman, 2010; Slater et al., 2010; Rabosky et al.  
551 2014). Although we still recover Delphindae as rapid radiation using a phylogeny of extant

552 and extinct cetaceans, we find support for strikingly different underlying dynamics. While  
553 there is still evidence for increased speciation rates in Delphinidae (Figs 6a; 7a), their  
554 elevated net diversification rates are predominantly driven by dramatically decreased  
555 extinction rates relative to other cetaceans (Figs 6b; 7b). One explanation for this finding  
556 could be that dolphins are in the early phase of adaptive radiation within an unoccupied  
557 adaptive zone, wherein speciation is rapid and extinction = 0 due to a lack of competition  
558 (Simpson, 1953; Valentine, 1980; Van Valen, 1985). However, Stanley (1990) has argued  
559 that, because so few clades break the strong correlation between origination and extinction  
560 rates, those that do (“Supertaxa”) likely possess uniquely advantageous combinations of  
561 life history traits, such as low dispersal rates combined with large population sizes,  
562 compared with related clades. The precise nature of the relationships that arise between  
563 traits and speciation / extinction dynamics are complex and mechanism dependent (see,  
564 for example, Table 1 in Jablonski, 2008) but it is notable that delphinids are social and  
565 ecologically flexible, while their diversification has previously been linked to  
566 Plio–Pleistocene changes in ocean currents that resulted in abrupt, localized, soft barriers  
567 to gene flow (do Amaral et al., 2018). A greater understanding of the multivariate  
568 structure of life history traits with Cetacea (e.g., Pianka et al., 2017) may reveal more  
569 insights into how Delphinidae has managed to break the speciation – extinction correlation  
570 with such dramatic effect.

### 571 *Paleo-Problems and Future Directions*

572 Any phylogenetic hypothesis is only as robust as the data from which it is inferred.  
573 Ultimately the onus is on the user to ensure that the data are of sufficient quality and  
574 independence that the resulting tree(s) stand up to scrutiny (Bininda-Emonds et al.,  
575 2004). By establishing a formalized set of rules for dealing with data re-use, recovery of  
576 multiple optimal trees, and the use of OTUs corresponding to different levels of the  
577 taxonomic hierarchy, the metatree pipeline (Lloyd et al., 2016) provides an explicit

578 framework for ameliorating some of the criticisms and concerns leveled at earlier MRP  
579 supertrees (Springer and de Jong, 2001; Gatesy et al., 2002, 2004; Gatesy and Springer,  
580 2004; Page, 2004). This is not to say that there are no concerns or areas for future  
581 improvement with our approach.

582 MRP supertrees have been criticized on the basis that they can recover unique  
583 clades that are not present in the profile of source trees (Wilkinson, 1995;  
584 Bininda-Emonds, 2003; Gatesy et al., 2004). Few unusual clades emerge in our strict  
585 consensus metatrees, but we do recover a unique Llanocetidae (Fig 5), consisting of  
586 *Llanocetus denticrenatus*, *Mystacodon selenensis*, *Niparajacetus palmidentis* and ZMT62 an  
587 undescribed taxon from New Zealand (Fordyce, 1989). *Mystacodon*'s placement is not a  
588 subject of concern; although the taxon was originally described as an earlier diverging  
589 mysticete (Lambert et al., 2017; de Muizon et al., 2019) its placement within Llanocetidae  
590 is in line with a number of recent studies (e.g., Fordyce and Marx, 2018; Marx et al., 2019;  
591 Azucena Solis-Añorve and Gerardo González-Barba and René Hernández-Rivera, 2019).  
592 The other two taxa have not been recovered as llanocetids in published sources  
593 incorporated here, but their placements can be easily explained. ZMT62 features in a  
594 single study, that of Geisler et al. (2017), and is figured (their Fig. 4) as the sister lineage  
595 to a clade consisting of Mammalodontidae + Aetiocetidae and ((*Llanocetus*,  
596 (Eomysticetidae, crown group mysticetes)). Inspection of the supplementary methods of  
597 Geisler et al. (2017) reveals that this topology is derived from an analysis using implied  
598 weights (Goloboff, 1993), a procedure that has been shown to increase resolution at the  
599 expense of accuracy (Congreve and Lamsdell, 2016), and that the authors' own analyses  
600 using equal weights yield a topology with ZMT62 as the sister taxon to *Llanocetus*, as we  
601 also found. The placement of *Niparajacetus* can be equally well explained. The original  
602 description of this taxon included a bootstrap consensus tree rooted sequentially by the  
603 archaeocete *Zygorhiza* and a selection of odontocetes, in which *Niparajacetus* is recovered  
604 in a polytomy with *Coronodon havensteini*, Mammalodontidae, Aetiocetidae,

605 Eomysticetidae and crown group mysticetes, and with Llanocetidae as sister to this clade  
606 (Azucena Solis-Añorve and Gerardo González-Barba and René Hernández-Rivera, 2019  
607 their Fig.7). Our reanalysis of the character matrix yields an identical topology with one  
608 exception: the odontocete outgroups are nested within mysticetes. Indeed, rerooting the  
609 tree on the odontocetes produces a topology in which *Niparajacetus* falls within a  
610 monophyletic Llanocetidae, consistent with our metatree results. The recovery of this  
611 previously unreported clade in the metatree can therefore be considered to result from  
612 careful scrutiny of the input data, rather than a compromise between conflicting  
613 relationships in figured topologies that might emerge from a traditional MRP supertree.

614 It is well understood that failing to account for unsampled taxa can bias inference  
615 of diversification dynamics based on molecular phylogenies (Pybus and Harvey, 2000;  
616 FitzJohn et al., 2009; Höhna et al., 2011). To overcome this issue, some authors have used  
617 random birth–death resolutions, combined with taxonomic constraints, to integrate over all  
618 possible placements of unsampled taxa (Kuhn et al., 2011). We used a similar procedure  
619 here to include unsampled fossil species by using the Paleobiology Database’s taxonomy as  
620 a down–weighted constraint during metatree inference. There are reasons to be concerned  
621 that this procedure may introduce a substantial source of error when inferring the  
622 placement of unsampled species. Although cetaceans possess one of the most well–curated  
623 set of records in the database (e.g., Uhen and Pyenson, 2007), a number of records of  
624 uncertain or doubtful status exist that have dramatic impacts on downstream analyses.  
625 For example, the Paleobiology Database records the taxon *Balaena dubusi* from the middle  
626 Miocene of Belgium (Louwey et al., 2010), in turn implying a minimum age of 15 Ma for  
627 the divergence of the sole extant member of the genus *Balaena*, the bowhead *B. mysticetus*  
628 from the right whales *Eubalaena*. In our GENUS and ALL analyses, inclusion of this taxon  
629 contributes to an increase in the mean age of crown group balaenids from 8.6 Ma in the  
630 EXCLUDE analysis to ~ 18 Ma (Table 1). *B. dubusi* was described by Van Beneden  
631 (1872) from a single vertebral column and Steeman (2010) has discussed the many issues

632 surrounding taxa described from the Antwerp faunas, considering many as *nomina dubia*.  
633 While the status of *B. dubusi* awaits formal re-assessment, it seems plausible that its  
634 assignment to the extant genus *Balaena* is in error. It is likely that similar taxonomic  
635 issues influence topology, branch lengths, and subsequent macroevolutionary inference in  
636 other parts of the GENUS and ALL trees (Figures 617). Notably, the inference of older  
637 divergence times for Delphinidae in these “more complete” trees than for the EXCLUDE  
638 analysis may provide an explanation for the loss of signal for increased diversification rates  
639 during the past 10 Ma. It should be noted that the birth–death polytomy resolution is not  
640 without issue in molecular phylogenetics either, resulting in elevated relative extinction  
641 rates ( $\mu / \lambda$ ), increased “tippy–ness” and more balanced trees than are found in empirical  
642 distributions of trees (Kuhn et al., 2011). The appropriate placement of unsampled extant  
643 taxa similarly depends on the accuracy of taxonomic constraints used. However, the fact  
644 that fossil taxa are non–contemporaneous means that they potentially exert more influence  
645 on divergence time estimates (Soul and Friedman, 2015). The inclusion of unsampled fossil  
646 taxa in meta–analytic phylogenies should always be carefully considered and justified and,  
647 at least for cetaceans, we recommend that the EXCLUDE trees should be the preferred  
648 hypotheses used in downstream analyses. More generally, these results emphasize that  
649 uncritical use of paleontological databases in phylogenetic and macroevolutionary research  
650 has the potential to produce flawed inferences and every taxon should, ideally, be vetted  
651 against the literature to corroborate its status.

652 A potential criticism of the metatree approach, as applied here, is that the resulting  
653 posterior distribution of time–scaled topologies does not explicitly incorporate topological  
654 uncertainty derived from the sample of input trees. Previous paleo–supertree studies have  
655 attempted to accommodate topological and divergence time uncertainty by first obtaining  
656 a subsample of most parsimonious trees and then using paleontological approaches to  
657 generate multiple sets of branch lengths per tree (e.g., Clarke et al., 2016; Lloyd et al.,  
658 2016). Although some phylogenetic uncertainty is propagated through our BEAST



659 analyses due to the use of the strict consensus metatree as a topological constraint, many  
660 nodes were fixed (for the EXCLUDE tree in particular) due to the well-resolved nature of  
661 the resulting estimate. Molecular phylogeneticists have employed a divide-and-conquer  
662 approach called “backbone-and-patch” (Jetz et al., 2012; Tonini et al., 2016; Jetz and  
663 Pyron, 2018; Upham et al., 2019), wherein topologies for densely sampled monophyletic  
664 subclades are pasted onto time-scaled higher-level topologies, to obtain a pseudo-posterior  
665 distribution of time-scaled topologies that can be used in comparative analyses.  
666 Logistically, such an approach cannot work in paleontological contexts because it would  
667 require assumptions of monophyly, which may vary between studies, and appropriate  
668 character taxon matrices for both the backbone and patch clades, which are also lacking in  
669 most cases. There is some cause to be optimistic that solutions can be found. Akanni et al.  
670 (2015) used Markov chain Monte Carlo to sample the posterior distribution of rooted  
671 supertree topologies under the exponential error model of Steel and Rodrigo (2008) and  
672 found that the approach performed well in terms of topology inference, clade support, and  
673 computation time. Efficient approaches for generating time-scaled trees of extinct taxa  
674 that also appropriately accommodate topological and branch length uncertainty will  
675 require similar Bayesian treatments.

### 676 *Conclusions*

677 Metatrees have some key benefits over traditional MRP supertrees that render them  
678 ideal for comparative paleobiologists. Complete sampling of taxa from the source data is  
679 always achieved, whereas a supertree can suffer when figured source trees collapse  
680 non-focal clades (loss of resolution) or key outgroups are excluded (loss of overlap).  
681 Additionally, a preferred method of inference (e.g., parsimony, maximum likelihood, or  
682 Bayesian inference) can be applied when re-analyzing the source data and a preferred  
683 output, such as a complete set of most parsimonious trees, maximum likelihood tree or  
684 sample from a Bayesian posterior distribution, can be used for metatree inference. This



685 latter step enables a more realistic inclusion of phylogenetic uncertainty in the resulting  
686 composite phylogeny than can be accomplished through the use of published consensus  
687 trees (see [Bell and Lloyd, 2015](#), their Figure 4). In other words, metatrees take more  
688 information forward from the source data to the synthetic hypothesis than traditional  
689 MRP supertrees do, and this tends to lead to better resolved topologies ([Lloyd et al.,  
690 2016](#)). Most importantly, and as our comparative analyses demonstrate, the ability to  
691 generate synthetic phylogenies containing large numbers of extinct taxa allows for the  
692 critical assessment of macroevolutionary hypotheses derived from extant taxa alone. Here,  
693 we showed that the apparent pulse of increased cetacean diversification during the past 10  
694 myr is driven more by reduced extinction rates than by increased speciation, a pattern  
695 long established in the fossil record but almost undetectable using extant species alone.  
696 While a supermatrix, with character states coded for every extinct species, remains a  
697 compelling standard for morphologists to strive for ([Gatesy and Springer, 2004](#)), supertrees  
698 realistically provide the most direct and accessible route for generating large phylogenies  
699 containing extinct taxa which, as simulations suggest ([Slater et al., 2012](#); [Louca and  
700 Pennell, 2020](#)) and our results show, are essential for obtaining accurate parameter  
701 estimates and model inference from macroevolutionary and macroecological analyses.

#### 702 ACKNOWLEDGEMENTS

703 We extend our sincere gratitude to Mark D. Uhen for his dedicated entry of  
704 cetacean fossil occurrences into the Paleobiology Database. Michael McGowan provided his  
705 molecular alignment and discussion of divergence times and the taxonomy of fossil  
706 cetaceans. Jon Hill wrote parallelization code for TNT. David Černý, Natalie Cooper,  
707 David Jablonski, Felix Marx, Rossy Natale, Mark Uhen, and Anna Wisniewski provided  
708 helpful comments and criticisms on early drafts of the manuscript. GTL was supported, in  
709 part, by a Researcher Mobility Award from the University of Leeds.

710

REFERENCES

- 711 Akanni, W. A., M. Wilkinson, C. J. Creevey, P. G. Foster, and D. Pisani. 2015.  
712 Implementing and testing bayesian and maximum-likelihood supertree methods in  
713 phylogenetics. *Royal Society open science* 2:140436.
- 714 Albert, J. S., D. M. Johnson, and J. H. Knouft. 2009. Fossils provide better estimates of  
715 ancestral body size than do extant taxa in fishes. *Acta Zoologica* 90:357–384.
- 716 Azucena Solis-Añorve and Gerardo González-Barba and René Hernández-Rivera. 2019.  
717 Description of a new toothed mysticete from the Late Oligocene of San Juan de La  
718 Costa, B.C.S., México. *Journal of South American Earth Sciences* 89:337 – 346.
- 719 Bajpai, S. and P. D. Gingerich. 1998. A new Eocene archaeocete (Mammalia, Cetacea)  
720 from India and the time of origin of whales. *Proceedings of the National Academy of*  
721 *Sciences* 95:15464–15468.
- 722 Baum, B. R. 1992. Combining trees as a way of combining data sets for phylogenetic  
723 inference, and the desirability of combining gene trees. *Taxon* Pages 3–10.
- 724 Baum, B. R. and M. A. Ragan. 2004. The mrp method. Pages 17–34 *in* *Phylogenetic*  
725 *supertrees*. Springer.
- 726 Beaulieu, J. M. and B. C. O’Meara. 2015. Extinction can be estimated from moderately  
727 sized molecular phylogenies. *Evolution* 69:1036–1043.
- 728 Beaulieu, J. M. and B. C. O’Meara. 2018. Can we build it? Yes we can, but should we use  
729 it? Assessing the quality and value of a very large phylogeny of campanulid angiosperms.  
730 *American Journal of Botany* 105:417–432.
- 731 Beaulieu, J. M. and B. C. O’Meara. 2019. Diversity and skepticism are vital for  
732 comparative biology: a response to Donoghue and Edwards (2019). *American Journal of*  
733 *Botany* 106:613–617.

- 734 Bell, M. A. and G. T. Lloyd. 2015. strap: an R package for plotting phylogenies against  
735 stratigraphy and assessing their stratigraphic congruence. *Palaeontology* 58:379–389.
- 736 Betancur-R, R., G. Ortí, and R. A. Pyron. 2015. Fossil-based comparative analyses reveal  
737 ancient marine ancestry erased by extinction in ray-finned fishes. *Ecology Letters*  
738 18:441–450.
- 739 Bininda-Emonds, O. 2004. *Phylogenetic supertrees: combining information to reveal the*  
740 *tree of life*. Springer Science & Business Media.
- 741 Bininda-Emonds, O. R., K. E. Jones, S. A. Price, M. Cardillo, R. Grenyer, and A. Purvis.  
742 2004. Garbage in, garbage out. Pages 267–280 *in* *Phylogenetic supertrees* (O. R.  
743 Bininda-Emonds, ed.). Springer.
- 744 Bininda-Emonds, O. R. P. 2003. Novel versus unsupported clades: Assessing the  
745 qualitative support for clades in mrp supertrees. *Systematic Biology* 52:839–848.
- 746 Bininda-Emonds, O. R. P., J. L. Gittleman, and M. A. Steel. 2002. The (super)tree of life:  
747 Procedures, problems, and prospects. *Annual Review of Ecology and Systematics*  
748 33:265–289.
- 749 Boersma, A. T., M. R. McCurry, and N. D. Pyenson. 2017. A new fossil dolphin  
750 *Dilophodelphis fordycei* provides insight into the evolution of supraorbital crests in  
751 Platanistoidea (Mammalia, Cetacea). *Royal Society Open Science* 4:170022.
- 752 Bouckaert, R., J. Heled, D. Kühnert, T. Vaughan, C.-H. Wu, D. Xie, M. A. Suchard,  
753 A. Rambaut, and A. J. Drummond. 2014. BEAST 2: a software platform for Bayesian  
754 evolutionary analysis. *PLoS Comput Biol* 10:e1003537.
- 755 Cantalapiedra, J. L., M. Hernández Fernández, B. Azanza, and J. Morales. 2015.  
756 Congruent phylogenetic and fossil signatures of mammalian diversification dynamics  
757 driven by Tertiary abiotic change. *Evolution* 69:2941–2953.

- 758 Churchill, M., M. Martinez-Caceres, C. de Muizon, J. Mnieckowski, and J. H. Geisler.  
759 2016. The origin of high-frequency hearing in whales. *Current Biology* 26:2144–2149.
- 760 Clarke, J. T., G. T. Lloyd, and M. Friedman. 2016. Little evidence for enhanced  
761 phenotypic evolution in early teleosts relative to their living fossil sister group.  
762 *Proceedings of the National Academy of Sciences* 113:11531–11536.
- 763 Congreve, C. R. and J. C. Lamsdell. 2016. Implied weighting and its utility in  
764 palaeontological datasets: a study using modelled phylogenetic matrices. *Palaeontology*  
765 59:447–462.
- 766 Cooney, C. R., J. A. Bright, E. J. Capp, A. M. Chira, E. C. Hughes, C. J. Moody, L. O.  
767 Nouri, Z. K. Varley, and G. H. Thomas. 2017. Mega-evolutionary dynamics of the  
768 adaptive radiation of birds. *Nature* 542:344–347.
- 769 de Muizon, C., G. Bianucci, M. Martínez-Cáceres, and O. Lambert. 2019. *Mystacodon*  
770 *selenensis*, the earliest known toothed mysticete (Cetacea, Mammalia) from the late  
771 Eocene of Peru: anatomy, phylogeny, and feeding adaptations. *Geodiversitas* 41:401 –  
772 499.
- 773 de Queiroz, A. and J. Gatesy. 2007. The supermatrix approach to systematics. *Trends in*  
774 *Ecology Evolution* 22:34 – 41.
- 775 do Amaral, K. B., A. R. Amaral, R. Ewan Fordyce, and I. B. Moreno. 2018. Historical  
776 Biogeography of Delphininae Dolphins and Related Taxa (Artiodactyla: Delphinidae).  
777 *Journal of Mammalian Evolution* 25:241–259.
- 778 Donoghue, M. J. and E. J. Edwards. 2019. Model clades are vital for comparative biology,  
779 and ascertainment bias is not a problem in practice: a response to Beaulieu and O’Meara  
780 (2018). *American Journal of Botany* 106:327–330.
- 781 Felsenstein, J. 1985. Phylogenies and the comparative method. *The American Naturalist*  
782 125:pp. 1–15.

- 783 Finarelli, J. A. and J. J. Flynn. 2006. Ancestral state reconstruction of body size in the  
784 Caniformia (Carnivora, Mammalia): The effects of incorporating data from the fossil  
785 record. *Systematic Biology* 55:301–313.
- 786 FitzJohn, R. G., W. P. Maddison, and S. P. Otto. 2009. Estimating trait-dependent  
787 speciation and extinction rates from incompletely resolved phylogenies. *Systematic*  
788 *Biology* 58:595–611.
- 789 Fleischauer, M. and S. Böcker. 2017. Bad clade deletion supertrees: A fast and accurate  
790 supertree algorithm. *Molecular Biology and Evolution* 34:2408–2421.
- 791 Foote, M. 1996. Models of morphological diversification. Pages 62–88 *in* *Evolutionary*  
792 *Paleobiology* (J. D., D. Erwin, and J. Lipps, eds.). University of Chicago Press.
- 793 Fordyce, R. E. 1989. Problematic Early Oligocene toothed whale (Cetacea,? Mysticeti)  
794 from Waikari, North Canterbury, New Zealand. *New Zealand Journal of Geology and*  
795 *Geophysics* 32:395–400.
- 796 Fordyce, R. E. and F. G. Marx. 2018. Gigantism precedes filter feeding in baleen whale  
797 evolution. *Current Biology* 28:1670 – 1676.e2.
- 798 Gatesy, J., R. H. Baker, and C. Hayashi. 2004. Inconsistencies in arguments for the  
799 supertree approach: Supermatrices versus supertrees of Crocodylia. *Systematic Biology*  
800 53:342–355.
- 801 Gatesy, J., C. Matthee, R. DeSalle, and C. Hayashi. 2002. Resolution of a  
802 supertree/supermatrix paradox. *Systematic Biology* 51:652–664.
- 803 Gatesy, J. and M. S. Springer. 2004. A critique of matrix representation with parsimony  
804 supertrees. Pages 369–388 *in* *Phylogenetic Supertrees*. Springer.
- 805 Gavryushkina, A., T. A. Heath, D. T. Ksepka, T. Stadler, D. Welch, and A. J. Drummond.  
806 2017. Bayesian total-evidence dating reveals the recent crown radiation of penguins.  
807 *Systematic Biology* 66:57–73.

- 808 Gavryushkina, A., D. Welch, T. Stadler, and A. J. Drummond. 2014. Bayesian inference of  
809 sampled ancestor trees for epidemiology and fossil calibration. *PLoS Comput Biol*  
810 10:e1003919.
- 811 Geisler, J. H., R. W. Boessenecker, M. Brown, and B. L. Beatty. 2017. The origin of filter  
812 feeding in whales. *Current Biology* 27:2036 – 2042.e2.
- 813 Gilinsky, N. L. 1994. Volatility and the Phanerozoic decline of background extinction  
814 intensity. *Paleobiology* 20:445–458.
- 815 Glor, R. E. 2010. Phylogenetic insights on adaptive radiation. *Annual Review of Ecology,  
816 Evolution, and Systematics* 41:251–270.
- 817 Godfrey, S. J., L. G. Barnes, and O. Lambert. 2017. The Early Miocene Odontocete  
818 *Araeodelphis natator* Kellogg, 1957 (Cetacea; Platanistidae), from the Calvert Formation  
819 of Maryland, U.S.A. *Journal of Vertebrate Paleontology* 37.
- 820 Goloboff, P. A. 1993. Estimating character weights during tree search. *Cladistics* 9:83–91.
- 821 Goloboff, P. A., J. S. Farris, and K. C. Nixon. 2008. TNT, a free program for phylogenetic  
822 analysis. *Cladistics* 24:774–786.
- 823 Hagen, O., T. Andermann, T. B. Quental, A. Antonelli, and D. Silvestro. 2017. Estimating  
824 Age-Dependent Extinction: Contrasting Evidence from Fossils and Phylogenies.  
825 *Systematic Biology* 67:458–474.
- 826 Harmon, L. J., J. B. Losos, T. Jonathan Davies, R. G. Gillespie, J. L. Gittleman,  
827 W. Bryan Jennings, K. H. Kozak, M. A. McPeck, F. Moreno-Roark, T. J. Near,  
828 A. Purvis, R. E. Ricklefs, D. Schluter, J. A. Schulte II, O. Seehausen, B. L. Sidlauskas,  
829 O. Torres-Carvajal, J. T. Weir, and A. Ø. Mooers. 2010. Early bursts of body size and  
830 shape evolution are rare in comparative data. *Evolution* 64:2385–2396.
- 831 Hartman, S., M. Mortimer, W. R. Wahl, D. R. Lomax, J. Lippincott, and D. M. Lovelace.

- 832 2019. A new paravian dinosaur from the Late Jurassic of North America supports a late  
833 acquisition of avian flight. *PeerJ* 7:e7247.
- 834 Harvey, P. H. and M. D. Pagel. 1991. *The Comparative Method in Evolutionary Biology*  
835 vol. 239. Oxford University Press Oxford.
- 836 Heath, T. A., J. P. Huelsenbeck, and T. Stadler. 2014. The fossilized birth–death process  
837 for coherent calibration of divergence-time estimates. *Proceedings of the National*  
838 *Academy of Sciences* 111:E2957–E2966.
- 839 Höhna, S., T. Stadler, F. Ronquist, and T. Britton. 2011. Inferring speciation and  
840 extinction rates under different sampling schemes. *Molecular Biology and Evolution*  
841 28:2577–2589.
- 842 Humphreys, A. and T. Barraclough. 2014. The evolutionary reality of higher taxa in  
843 mammals. *Proceedings of the Royal Society B-Biological Sciences* 281.
- 844 Hunt, G. and G. Slater. 2016. Integrating paleontological and phylogenetic approaches to  
845 macroevolution. *Annual Review of Ecology, Evolution, and Systematics* 47:189–213.
- 846 Jablonski, D. 2008. Species selection: Theory and data. *Annual Review of Ecology,*  
847 *Evolution, and Systematics* 39:501–524.
- 848 Jablonski, D., J. J. Sepkoski, D. J. Bottjer, and P. M. Sheenan. 1983. Onshore-offshore  
849 patterns in the evolution of Phanerozoic shelf communities. *Science* 222:1123–1125.
- 850 Jetz, W. and R. A. Pyron. 2018. The interplay of past diversification and evolutionary  
851 isolation with present imperilment across the amphibian tree of life. *Nature Ecology &*  
852 *Evolution* 2:850–858.
- 853 Jetz, W., G. H. Thomas, J. B. Joy, K. Hartmann, and A. O. Mooers. 2012. The global  
854 diversity of birds in space and time. *Nature* 491:444 EP –.

- 855 Kettleborough, G., J. Dicks, I. N. Roberts, and K. T. Huber. 2015. Reconstructing  
856 (Super)Trees from Data Sets with Missing Distances: Not All Is Lost. *Molecular Biology*  
857 *and Evolution* 32:1628–1642.
- 858 Knope, M. L., A. M. Bush, L. O. Frishkoff, N. A. Heim, and J. L. Payne. 2020. Ecologically  
859 diverse clades dominate the oceans via extinction resistance. *Science* 367:1035–1038.
- 860 Kuhn, T. S., A. Ø. Mooers, and G. H. Thomas. 2011. A simple polytomy resolver for dated  
861 phylogenies. *Methods in Ecology and Evolution* 2:427–436.
- 862 Labandeira, C. and J. Sepkoski. 1993. Insect diversity in the fossil record. *Science*  
863 261:310–315.
- 864 Lambert, O., G. Bianucci, and M. Urbina. 2014. *Huaridelphis raimondii*, a new early  
865 Miocene Squalodelphinidae (Cetacea, Odontoceti) from the Chilcatay Formation, Peru.  
866 *Journal of Vertebrate Paleontology* 34:987–1004.
- 867 Lambert, O., M. Martínez-Cáceres, G. Bianucci, C. D. Celma], R. Salas-Gismondi,  
868 E. Steurbaut, M. Urbina, and C. [de Muizon]. 2017. Earliest mysticete from the Late  
869 Eocene of Peru sheds new light on the origin of baleen whales. *Current Biology* 27:1535  
870 – 1541.e2.
- 871 Law, C. J., G. J. Slater, and R. S. Mehta. 2017. Lineage diversity and size disparity in  
872 Musteloidea: Testing patterns of adaptive radiation using molecular and fossil-based  
873 methods. *Systematic Biology* 67:127–144.
- 874 Levasseur, C. and F.-J. Lapointe. 2006. Total evidence, average consensus and matrix  
875 representation with parsimony: What a difference distances make. *Evolutionary*  
876 *bioinformatics online* 2:1.
- 877 Lin, H. T., J. G. Burleigh, and O. Eulenstein. 2009. Triplet supertree heuristics for the tree  
878 of life. *BMC Bioinformatics* 10:S8.



- 879 Liow, L. H., T. B. Quental, and C. R. Marshall. 2010. When Can Decreasing  
880 Diversification Rates Be Detected with Molecular Phylogenies and the Fossil Record?  
881 *Systematic Biology* 59:646–659.
- 882 Lloyd, G. T. 2016. Estimating morphological diversity and tempo with discrete  
883 character-taxon matrices: implementation, challenges, progress, and future directions.  
884 *Biological Journal of the Linnean Society* 118:131–151.
- 885 Lloyd, G. T., D. W. Bapst, M. Friedman, and K. E. Davis. 2016. Probabilistic divergence  
886 time estimation without branch lengths: dating the origins of dinosaurs, avian flight and  
887 crown birds. *Biology Letters* 12:20160609.
- 888 Lloyd, G. T., K. E. Davis, D. Pisani, J. E. Tarver, M. Ruta, M. Sakamoto, D. W. E. Hone,  
889 R. Jennings, and M. J. Benton. 2008. Dinosaurs and the Cretaceous terrestrial  
890 revolution. *Proceedings of the Royal Society B* 275:2483–2490.
- 891 Losos, J. B. 2009. *Lizards in an Evolutionary Tree: Ecology and Adaptive Radiation of*  
892 *Anoles*. University of California Press, Berkeley.
- 893 Louca, S. and M. W. Pennell. 2020. Extant timetrees are consistent with a myriad of  
894 diversification histories. *Nature* 580:502–505.
- 895 Louwye, S., R. Marquet, M. Bosselaers, and O. Lambert. 2010. Stratigraphy of an  
896 early–middle Miocene sequence near Antwerp in northern Belgium (southern north sea  
897 basin). *Geologica Belgica* 13:269–284.
- 898 Marshall, C. R. 2017. Five palaeobiological laws needed to understand the evolution of the  
899 living biota. *Nature Ecology & Evolution* 1:0165.
- 900 Martin, C. H. and E. J. Richards. 2019. The paradox behind the pattern of rapid adaptive  
901 radiation: How can the speciation process sustain itself through an early burst? *Annual*  
902 *Review of Ecology, Evolution, and Systematics* 50:569–593.

- 903 Marx, F. G. and R. E. Fordyce. 2015. Baleen boom and bust: a synthesis of mysticete  
904 phylogeny, diversity and disparity. *Royal Society Open Science* 2:140434.
- 905 Marx, F. G., K. Post, M. Bosselaers, and D. K. Munsterman. 2019. A large Late Miocene  
906 cetotheriid (Cetacea, Mysticeti) from the Netherlands clarifies the status of  
907 *Tranatocetidae*. *PeerJ* 7:e6426.
- 908 McGowen, M. R., M. Spaulding, and J. Gatesy. 2009. Divergence date estimation and a  
909 comprehensive molecular tree of extant cetaceans. *Molecular Phylogenetics and*  
910 *Evolution* 53:891 – 906.
- 911 McGowen, M. R., G. Tsagkogeorga, S. Álvarez-Carretero, M. dos Reis, M. Struebig,  
912 R. Deaville, P. D. Jepson, S. Jarman, A. Polanowski, P. A. Morin, and S. J. Rossiter.  
913 2019. Phylogenomic Resolution of the Cetacean Tree of Life Using Target Sequence  
914 Capture. *Systematic Biology* Syz068.
- 915 McMahan, M. M. and M. J. Sanderson. 2006. Phylogenetic Supermatrix Analysis of  
916 GenBank Sequences from 2228 Papilionoid Legumes. *Systematic Biology* 55:818–836.
- 917 Mead, J. G. and R. L. Brownell Jr. 1993. Order cetacea. Pages 723–743 *in* *Mammal*  
918 *species of the world: a taxonomic and geographic reference* (D. E. Wilson and D. M.  
919 Reeder, eds.) 3rd ed. The Johns Hopkins University Press.
- 920 Meseguer, A. S., J. M. Lobo, R. Ree, D. J. Beerling, and I. Sanmartín. 2014. Integrating  
921 Fossils, Phylogenies, and Niche Models into Biogeography to Reveal Ancient  
922 Evolutionary History: The Case of *Hypericum* (Hypericaceae). *Systematic Biology*  
923 64:215–232.
- 924 Miller, M., W. Pfeiffer, and T. Schwartz. 2010. Creating the CIPRES science gateway for  
925 inference of large phylogenetic trees. Pages 1 – 8 *in* *Proceedings of the the gateway*  
926 *computing environments workshop (GCE)*, 14 Nov. 2010, New Orleans, LA.

- 927 Mitchell, J. S., R. S. Etienne, and D. L. Rabosky. 2018. Inferring Diversification Rate  
928 Variation From Phylogenies With Fossils. *Systematic Biology* 68:1–18.
- 929 Mo, J.-y., X. Xu, and S. E. Evans. 2012. A large predatory lizard (Platynota, Squamata)  
930 from the Late Cretaceous of South China. *Journal of Systematic Palaeontology*  
931 10:333–339.
- 932 Morlon, H., T. L. Parsons, and J. B. Plotkin. 2011. Reconciling molecular phylogenies with  
933 the fossil record. *Proceedings of the National Academy of Sciences* 108:16327.
- 934 Nguyen, N., S. Mirarab, and T. Warnow. 2012. MRL and SuperFine+MRL: new supertree  
935 methods. *Algorithms for Molecular Biology* 7:3.
- 936 O’Leary, M. A. and S. Kaufman. 2011. Morphobank: phylophenomics in the ‘cloud’.  
937 *Cladistics* 27:1–9.
- 938 O’Meara, B. C., C. Ané, M. J. Sanderson, and P. C. Wainwright. 2006. Testing for  
939 different rates of continuous trait evolution using likelihood. *Evolution* 60:922–933.
- 940 Page, R. D. 2004. Taxonomy, supertrees, and the tree of life. Pages 247–265 *in*  
941 *Phylogenetic Supertrees*. Springer.
- 942 Peters, S. E. and M. McClellan. 2016. The Paleobiology Database application  
943 programming interface. *Paleobiology* 42:1–7.
- 944 Pianka, E. R., L. J. Vitt, N. Pelegrin, D. B. Fitzgerald, and K. O. Winemiller. 2017.  
945 Toward a periodic table of niches, or exploring the lizard niche hypervolume. *The*  
946 *American Naturalist* 190:601–616.
- 947 Pisani, D. and M. Wilkinson. 2002. Matrix representation with parsimony, taxonomic  
948 congruence, and total evidence 51:151–155.
- 949 Plummer, M., N. Best, K. Cowles, and K. Vines. 2006. CODA: Convergence Diagnosis and  
950 Output Analysis for MCMC. *R News* 6:7–11.

- 951 Pybus, O. G. and P. H. Harvey. 2000. Testing macro-evolutionary models using incomplete  
952 molecular phylogenies. *Proceedings of the Royal Society of London. Series B: Biological*  
953 *Sciences* 267:2267–2272.
- 954 Quental, T. B. and C. R. Marshall. 2010. Diversity dynamics: molecular phylogenies need  
955 the fossil record. *Trends in Ecology & Evolution* 25:434–441.
- 956 R Development Core Team. 2019. R: A Language and Environment for Statistical  
957 Computing. R Foundation for Statistical Computing Vienna, Austria ISBN  
958 3-900051-07-0.
- 959 Rabosky, D. L. 2010. Extinction rates should not be estimated from molecular phylogenies.  
960 *Evolution* 64:1816–1824.
- 961 Rabosky, D. L. 2014. Automatic detection of key innovations, rate shifts, and  
962 diversity-dependence on phylogenetic trees. *PLOS ONE* 9:1–15.
- 963 Rabosky, D. L., J. Chang, P. O. Title, P. F. Cowman, L. Sallan, M. Friedman,  
964 K. Kaschner, C. Garilao, T. J. Near, M. Coll, and M. E. Alfaro. 2018. An inverse  
965 latitudinal gradient in speciation rate for marine fishes. *Nature* 559:392–395.
- 966 Rabosky, D. L. and E. E. Goldberg. 2015. Model Inadequacy and Mistaken Inferences of  
967 Trait-Dependent Speciation. *Systematic Biology* 64:340–355.
- 968 Rabosky, D. L., M. Grundler, C. Anderson, P. Title, J. J. Shi, J. W. Brown, H. Huang,  
969 and J. G. Larson. 2014. BAMM tools: an R package for the analysis of evolutionary  
970 dynamics on phylogenetic trees. *Methods in Ecology and Evolution* 5:701–707.
- 971 Ragan, M. A. 1992. Phylogenetic inference based on matrix representation of trees.  
972 *Molecular phylogenetics and evolution* 1:53–58.
- 973 Ranwez, V., A. Criscuolo, and E. J. Douzery. 2010. SuperTriplets: a triplet-based supertree  
974 approach to phylogenomics. *Bioinformatics* 26:i115–i123.

- 975 Raup, D. M. 1994. The role of extinction in evolution. *Proceedings of the National*  
976 *Academy of Sciences* 91:6758–6763.
- 977 Ree, R. H. and S. A. Smith. 2008. Maximum likelihood inference of geographic range  
978 evolution by dispersal, local extinction, and cladogenesis. *Systematic Biology* 57:4–14.
- 979 Ronquist, F., M. Teslenko, P. Van Der Mark, D. L. Ayres, A. Darling, S. Höhna,  
980 B. Larget, L. Liu, M. A. Suchard, and J. P. Huelsenbeck. 2012. MrBayes 3.2: efficient  
981 Bayesian phylogenetic inference and model choice across a large model space. *Systematic*  
982 *biology* 61:539–542.
- 983 Sanderson, M. J. and A. C. Driskell. 2003. The challenge of constructing large phylogenetic  
984 trees. *Trends in Plant Science* 8:374–379.
- 985 Sanderson, M. J., A. Purvis, and C. Henze. 1998. Phylogenetic supertrees: Assembling the  
986 trees of life. *Trends in Ecology & Evolution* 13:105 – 109.
- 987 Schluter, D. 2000. *The Ecology of Adaptive Radiation*. Oxford University Press.
- 988 Semple, C., P. Daniel, W. Hordijk, R. D. Page, and M. Steel. 2004. Supertree algorithms  
989 for ancestral divergence dates and nested taxa. *Bioinformatics* 20:2355–2360.
- 990 Simpson, C., W. Kiessling, H. Mewis, R. C. Baron-Szabo, and J. Müller. 2011.  
991 Evolutionary diversification of reef corals: A comparison of the molecular and fossil  
992 records. *Evolution* 65:3274–3284.
- 993 Simpson, G. G. 1944. *Tempo and Mode in Evolution*. Columbia University Press.
- 994 Simpson, G. G. 1953. *Major Features of Evolution*. Columbia University Press.
- 995 Slater, G. J. and A. R. Friscia. 2019. Hierarchy in adaptive radiation: A case study using  
996 the Carnivora (Mammalia). *Evolution* 73:524–539.

- 997 Slater, G. J., J. A. Goldbogen, and N. D. Pyenson. 2017. Independent evolution of baleen  
998 whale gigantism linked to Plio-Pleistocene ocean dynamics. *Proceedings of the Royal*  
999 *Society of London B: Biological Sciences* 284.
- 1000 Slater, G. J., L. J. Harmon, and M. E. Alfaro. 2012. Integrating fossils with molecular  
1001 phylogenies improves inference of trait evolution. *Evolution* 66:3931–3944.
- 1002 Slater, G. J., S. A. Price, F. Santini, and M. E. Alfaro. 2010. Diversity versus disparity and  
1003 the radiation of modern cetaceans. *Proceedings of the Royal Society B-Biological*  
1004 *Sciences* 277:3097–3104.
- 1005 Smith, S. A., J. M. Beaulieu, and M. J. Donoghue. 2009. Mega-phylogeny approach for  
1006 comparative biology: an alternative to supertree and supermatrix approaches. *BMC*  
1007 *Evolutionary Biology* 9:37.
- 1008 Smith, S. A. and J. W. Brown. 2018. Constructing a broadly inclusive seed plant  
1009 phylogeny. *American Journal of Botany* 105:302–314.
- 1010 Smith, S. A., J. W. Brown, and J. F. Walker. 2018. So many genes, so little time: A  
1011 practical approach to divergence-time estimation in the genomic era. *PLOS ONE*  
1012 13:1–18.
- 1013 Soul, L. C. and M. Friedman. 2015. Taxonomy and phylogeny can yield comparable results  
1014 in comparative paleontological analyses. *Systematic Biology* 64:608–620.
- 1015 Springer, M. S. and W. W. de Jong. 2001. Which mammalian supertree to bark up?  
1016 *Science* 291:1709–1711.
- 1017 Stamatakis, A. 2014. Raxml version 8: a tool for phylogenetic analysis and post-analysis of  
1018 large phylogenies. *Bioinformatics* 30:1312–1313.
- 1019 Stanley, S. M. 1979. *Macroevolution, pattern and process*. Johns Hopkins University Press.

- 1020 Stanley, S. M. 1990. The general correlation between rate of speciation and rate of  
1021 extinction: fortuitous causal linkages. Pages 103–127 *in* Causes of evolution: a  
1022 Paleontological Perspective (R. Ross and W. Allmon, eds.). University of Chicago Press,  
1023 Chicago.
- 1024 Steel, M. and A. Rodrigo. 2008. Maximum likelihood supertrees. *Systematic biology*  
1025 57:243–250.
- 1026 Steeman, M. E. 2010. The extinct baleen whale fauna from the Miocene-Pliocene of  
1027 Belgium and the diagnostic cetacean ear bones. *Journal of Systematic Palaeontology*  
1028 8:63–80.
- 1029 Steeman, M. E., M. B. Hebsgaard, R. E. Fordyce, S. Y. W. Ho, D. L. Rabosky, R. Nielsen,  
1030 C. Rahbek, H. Glenner, M. V. Sørensen, and E. Willerslev. 2009. Radiation of Extant  
1031 Cetaceans Driven by Restructuring of the Oceans. *Systematic Biology* 58:573–585.
- 1032 Stroud, J. T. and J. B. Losos. 2016. Ecological opportunity and adaptive radiation. *Annual*  
1033 *Review of Ecology, Evolution, and Systematics* 47:507–532.
- 1034 Swenson, M. S., R. Suri, C. R. Linder, and T. Warnow. 2012. Superfine: Fast and accurate  
1035 supertree estimation. *Systematic Biology* 61:214–227.
- 1036 Tonini, J. F. R., K. H. Beard, R. B. Ferreira, W. Jetz, and R. A. Pyron. 2016.  
1037 Fully-sampled phylogenies of squamates reveal evolutionary patterns in threat status.  
1038 *Biological Conservation* 204:23 – 31.
- 1039 Uhen, M. D. 2008. New protocetid whales from alabama and mississippi, and a new  
1040 cetacean clade, Pelagiceti. *Journal of Vertebrate Paleontology* 28:589–593.
- 1041 Uhen, M. D. and N. D. Pyenson. 2007. Diversity estimates, biases, and historiographic  
1042 effects: resolving cetacean diversity in the tertiary. *Palaeontologia Electronica*  
1043 10:11A:22p.

- 1044 Upham, N. S., J. A. Esselstyn, and W. Jetz. 2019. Inferring the mammal tree: Species-level  
1045 sets of phylogenies for questions in ecology, evolution, and conservation. *PLOS Biology*  
1046 17:1–44.
- 1047 Valentine, J. W. 1980. Determinants of diversity in higher taxonomic categories.  
1048 *Paleobiology* 6:444–450.
- 1049 Valentine, J. W. 1990. The fossil record: a sampler of life’s diversity. *Phil. Trans. Roy. Soc.*  
1050 *Lond. B* 330:261–268.
- 1051 Van Beneden, P. J. 1872. Les Baleines fossiles d’Anvers. *Bulletins de L’Academie Royale*  
1052 *des Sciences, des Lettres et des Beaux-arts* 34:6–23.
- 1053 Van Valen, L. 1971. Adaptive zones and the orders of mammals. *Evolution* 25:420–428.
- 1054 Van Valen, L. M. 1985. A theory of origination and extinction. *Evolutionary Theory*  
1055 7:133–142.
- 1056 Varga, T., K. Krizsán, C. Földi, B. Dima, M. Sánchez-García, S. Sánchez-Ramírez, G. J.  
1057 Szöllösi, J. G. Szarkándi, V. Papp, L. Albert, W. Andreopoulos, C. Angelini, V. Antonín,  
1058 K. W. Barry, N. L. Bougher, P. Buchanan, B. Buyck, V. Bense, P. Catcheside,  
1059 M. Chovatia, J. Cooper, W. Dämon, D. Desjardin, P. Finy, J. Geml, S. Haridas,  
1060 K. Hughes, A. Justo, D. Karasiński, I. Kautmanova, B. Kiss, S. Kocsubé, H. Kotiranta,  
1061 K. M. LaButti, B. E. Lechner, K. Liimatainen, A. Lipzen, Z. Lukács, S. Mihaltcheva,  
1062 L. N. Morgado, T. Niskanen, M. E. Noordeloos, R. A. Ohm, B. Ortiz-Santana,  
1063 C. Ovrebo, N. Rácz, R. Riley, A. Savchenko, A. Shiryayev, K. Soop, V. Spirin,  
1064 C. Szebenyi, M. Tomšovský, R. E. Tulloss, J. Uehling, I. V. Grigoriev, C. Vágvölgyi,  
1065 T. Papp, F. M. Martin, O. Miettinen, D. S. Hibbett, and L. Nagy. 2019. Megaphylogeny  
1066 resolves global patterns of mushroom evolution. *Nature Ecology & Evolution* 3:668–678.
- 1067 Wilkinson, M. 1995. Coping with abundant missing entries in phylogenetic inference using  
1068 parsimony. *Systematic Biology* 44:501–514.



REFERENCES

49

- 1069 Wilkinson, M., D. Pisani, J. A. Cotton, and I. Corfe. 2005. Measuring Support and  
1070 Finding Unsupported Relationships in Supertrees. *Systematic Biology* 54:823–831.
- 1071 Zanne, A. E., D. C. Tank, W. K. Cornwell, J. M. Eastman, S. A. Smith, R. G. FitzJohn,  
1072 D. J. McGlinn, B. C. O’Meara, A. T. Moles, P. B. Reich, D. L. Royer, D. E. Soltis, P. F.  
1073 Stevens, M. Westoby, I. J. Wright, L. Aarssen, R. I. Bertin, A. Calaminus, R. Govaerts,  
1074 F. Hemmings, M. R. Leishman, J. Oleksyn, P. S. Soltis, N. G. Swenson, L. Warman, and  
1075 J. M. Beaulieu. 2014. Three keys to the radiation of angiosperms into freezing  
1076 environments. *Nature* 506:89–92.